Electronic Supplementary Material (ESI) for ChemComm.

The Supplementary Information for

A Twisted Macrocyclic Hexanuclear Palladium Complex with Internal Bulky Coordinating Ligands

Akira Nagai, Takashi Nakamura, Tatsuya Nabeshima

Graduate School of Pure and Applied Sciences

and Tsukuba Research Center for Energy Materials Science (TREMS),

University of Tsukuba, 1-1-1 Tennodai, Tsukuba, Ibaraki 305-8571, Japan

*Corresponding Author. E-mail: nabesima@chem.tsukuba.ac.jp

Contents

Materials and methods

Unless otherwise noted, the solvents and reagents were purchased from TCI Co., Ltd., FUJIFILM Wako Pure Chemical Industries, Ltd., Kanto Chemical Co., Inc., Nacalai Tesque, Inc. or Sigma-Aldrich Co., and used without further purification. Dry DMF was purified by Nikko Hansen Ultimate Solvent System 3S-TCN 1. Silica gel for column chromatography was purchased from Kanto Chemical Co. Inc. (Silica Gel 60 N (spherical, 63–210 μm or 40–50 μm). Alumina for column chromatography was purchased from FUJIFILM Wako Pure Chemical Industries, Ltd. (alumina, activated (about 75 μm)). GPC purification was performed by a JAI LC-9210 II NEXT system with JAIGEL-1HH/2HH columns using $CHCl_3$ as the eluent.

Measurements were performed at 298 K unless otherwise noted. ^{1}H, ^{13}C, ^{11}B, ^{19}F, and other 2D NMR spectra were recorded by a Bruker AVANCE III-600 (600 MHz) spectrometer or a Bruker AVANCE III-400 (400 MHz) spectrometer. The assignment of ^{1}H and ^{13}C signals were based on ^{1}H-^{1}H COSY, ^{1}H-^{1}H NOESY, ^{1}H-^{13}C HSQC, and ^{1}H-^{13}C HMBC measurements. Negative values were depicted in red in the spectra. Tetramethylsilane was used as the internal standard (δ 0.00 ppm) for the ^{1}H and ^{13}C NMR measurements when $CDCl_3$ was used as the solvent. When CD_3CN was used, residual solvent signals were used for the ^{1}H (δ 1.94 ppm) and ^{13}C NMR (δ 118.3 ppm) measurements.[S1] When DMSO-d_6 was used, residual solvent signals were used for the ^{1}H (δ 2.50 ppm) and ^{13}C NMR (δ 39.52 ppm) measurements.[S1] $BF_3{\cdot}Et_2O$ in $CDCl_3$ (1 wt%) was used as the external standard (δ 0.0 ppm) for the ^{11}B NMR measurements. Hexafluorobenzene in $CDCl_3$ (1 wt%) was used as the external standard (δ –163.0 ppm) for the ^{19}F NMR measurements.

The MALDI-TOF mass data were recorded by an AB SCIEX TOF/TOF 5800 system. The ESI-TOF mass data were recorded by a Waters SYNAPT G2 HDMS system or an AB SCIEX TripleTOF 4600 system.

The UV-Vis spectra were recorded on a JASCO V-670 spectrophotometer. The emission spectra were recorded by a JASCO FP-8600 fluorescence spectrophotometer. The absolute fluorescence quantum yields were determined by a Hamamatsu Photonics absolute PL quantum yield measurement system C9920-02. The solvents used for the measurements were air-saturated. The IR spectra were recorded by a JASCO FT/IR-480Plus spectrometer. The CD spectra were recorded by a JASCO J-820 spectrophotometer.

Single-crystal X-ray crystallographic measurement was performed using a Bruker APEX II ULTRA with MoKα radiation (graphite-monochromated, λ = 0.71073 Å) at 120 K. The collected diffraction images were processed by a Bruker APEX2. The initial structure was solved using SHELXS-97[S2] and refined using SHELXL-2014[S3], which were running on Yadokari-XG crystallographic software[S4]. CCDC 1881523 contains the data for this paper. The data can be obtained free of charge from The Cambridge Crystallographic Data Centre via www.ccdc.cam.ac.uk/getstructures.

MM calculations were performed by the Gaussian16[S5] with the UFF force field[S6]. QEq charges[S7] were used for all atoms. DFT calculations were performed by the Gaussian16[S5] with the B3LYP function in an acetonitrile environment. The basis set 6-31+G(d) was used for C, H, N, and O and the basis set LanL2DZ was used for Pd in geometry optimization and time-dependent calculations.

Melting points were determined by a Yanaco MP-J3 melting point apparatus. The elemental analysis was performed by a Yanaco MT-6 analyzer with tin boats purchased from Elementar. We appreciate Mr. Ikuo Iida and Mr. Masao Sasaki of the University of Tsukuba for the elemental analyses.

Synthesis and characterization of the compounds

Scheme S1. Synthesis of **4**[S8]

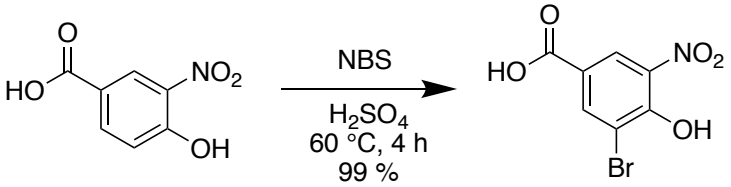

3 **4**

A solution of **3** (18.65 g, 101.9 mmol, 1.0 eq.) and NBS (22.1916 g, 124.7 mmol, 1.2 eq.) in H_2SO_4 (200 mL) was stirred at 60 °C for 4 h, and then added to an ice bath (2 L). The reaction mixture was filtered, and the solid was washed with water until the pH of the filtrate became neutral. The solid was dried in vacuo to give **4** (26.37 g, 100.7 mmol, 99%) as a yellow solid.

^{1}H NMR (600 MHz, DMSO-d_6): δ 8.39 (d, J = 2.1 Hz, 1H), 8.31 (d, J = 2.1 Hz, 1H);

^{13}C NMR (151 MHz, DMSO-d_6): δ 164.4, 152.6, 138.3, 137.0, 125.8, 122.4, 114.0;

m.p.: decomp. at 190 °C;

Elemental analysis: calcd for $C_7H_{4.6}NO_{5.3}Br$ (**4**·0.3H_2O); H, 1.73; C, 31.44; N, 5.24. found H, 1.40; C, 31.39; N, 5.03.

Scheme S2. Synthesis of **5**

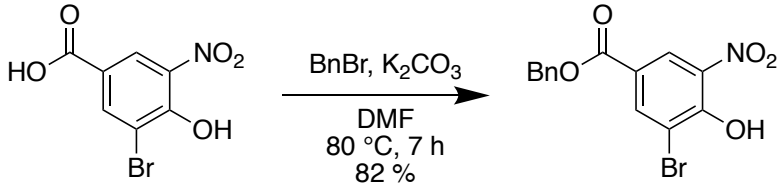

4 **5**

To a mixture of **4** (26.26 g, 100.2 mmol, 1.0 eq.) and K_2CO_3 (27.63 g, 199.93 mmol, 2.0 eq.) in dry DMF (260 mL) was added benzyl bromide (24 mL, 200 mmol, 2.0 eq.). The mixture was stirred at 80 °C for 7 h. The insolubles were removed by filtration and the filtrate was concentrated in vacuo. H_2O (100 mL) and 2 M HClaq (220 mL) was added to the crude, and the aqueous layer was extracted with EtOAc (300 mL × 1, then 100 mL × 2). The organic layer was dried over Na_2SO_4, filtered, and concentrated in vacuo. The residue was washed with hexane thoroughly, and dried in vacuo to give **5** as a pale yellow solid (28.93 g, 82.15 mmol, 82%).

^{1}H NMR (600 MHz, DMSO-d_6): δ 8.41 (d, J = 2.1 Hz, 1H), 8.33 (d, J = 2.1 Hz, 1H), 7.47 (d, J = 7.3 Hz, 2H), 7.40 (dd, J = 7.3, 7.3 Hz, 2H), 7.36 (t, J = 7.3 Hz, 1H);

^{13}C NMR (151 MHz, DMSO-d_6): δ 163.4, 153.7, 138.5, 137.7, 136.2, 129.0, 128.72, 128.60, 126.4, 121.4, 114.9, 67.3;

m.p.: 114.6–114.9 °C;

Elemental analysis: calcd for $C_{14}H_{10}BrNO_5$ (**5**); H, 2.86; C, 47.75; N, 3.98. found H, 2.83; C, 47.87; N, 3.94.

Scheme S3. Synthesis of **7**

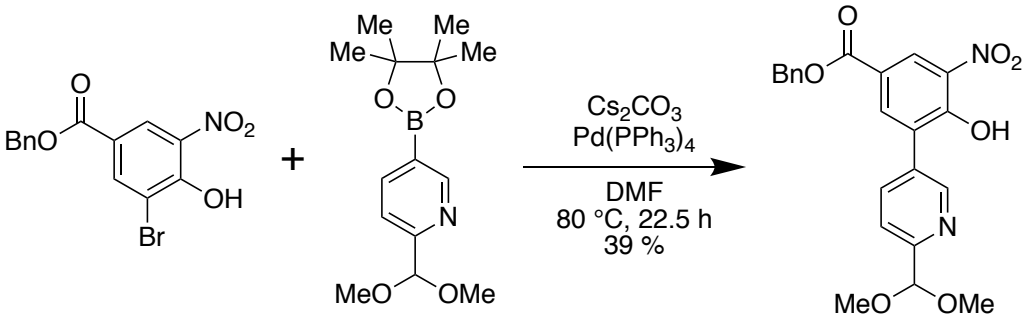

5 **6** **7**

To a mixture of **5** (12.54 g, 35.6 mmol, 1.0 eq.), **6**[S9] (12.23 g, 43.97 mmol, 1.2 eq.), and Cs_2CO_3 (52.80 g, 162.1 mmol, 4.6 eq.) in dry DMF (90 mL) was added $Pd(PPh_3)_4$ (1.707 g, 1.48 mmol, 4.1 mol%), and the mixture was stirred at 80 °C for 22.5 h under Ar atmosphere. The reaction mixture was concentrated in vacuo. H_2O (400 mL) was added to the residue, and the aqueous layer was extracted with CH_2Cl_2 (200 mL × 1, then 100 mL × 2). The organic layer was dried over Na_2SO_4, filtered, and concentrated in vacuo. The residue was purified by column chromatography on alumina (CH_2Cl_2/MeOH = 100/0–50/50) to give **7** as a red deliquescent sticky solid (5.945 g, 14 mmol, 39 %, calculated as free acid).

^{1}H NMR (600 MHz, $CDCl_3$): δ 11.46 (br, 1H), 8.89 (d, J = 2.1 Hz, 1H), 8.80 (d, J = 2.0 Hz, 1H), 8.32 (d, J = 2.1 Hz, 1H), 7.97 (dd, J = 8.1, 2.0 Hz, 1H), 7.67 (d, J = 8.1 Hz, 1H), 7.45 (d, J = 7.4 Hz, 2H), 7.40 (dd, J = 7.4 Hz, 2H), 7.36 (m, 1H), 5.45 (s, 1H), 5.40 (s, 2H), 3.46 (s, 6H);

^{13}C NMR (151 MHz, $CDCl_3$): δ 163.9, 157.2, 155.8, 149.1, 138.3, 137.4, 135.3, 133.9, 130.6, 129.7, 128.72, 128.61, 128.46, 127.1, 122.5, 120.8, 103.7, 67.5, 53.8;

m.p.: decomp. at 250 °C;

HRMS (ESI): *m/z* calcd for ([**7**·H$^+$]): 425.1349; found: 425.1324.

Scheme S4. Synthesis of **8**

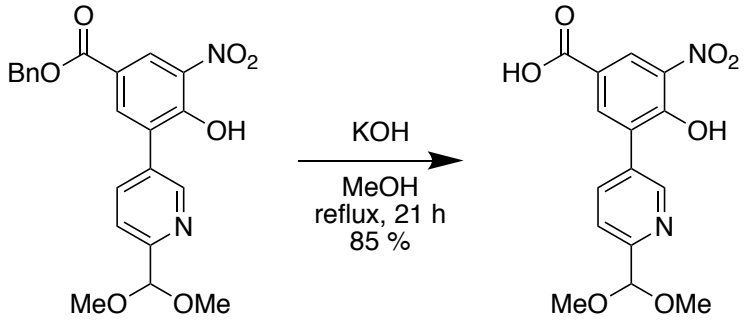

7 **8**

A mixture of **7** (4.006 g, 9.44 mmol, 1.0 eq.) and KOH (7.6501 g, 136.34 mmol, 14.4 eq.) in MeOH (150 mL) was refluxed for 21 h. The reaction mixture was concentrated in vacuo. H_2O was added to the residue, and the aqueous layer was washed with CH_2Cl_2 (20 mL × 3). 12 M HCl aq (10 mL) and 2 M HCl aq (5 mL) was added to the aqueous layer, after which yellow precipitation was formed. The solid was filtered, washed with water, and dried in vacuo to give **8** as a yellow solid (2.6938 g, 8.06 mmol, 85 %).

^{1}H NMR (600 MHz, DMSO-d_6): δ 8.74 (d, J = 2.0 Hz, 1H), 8.50 (d, J = 2.2 Hz, 1H), 8.12 (d, J = 2.2 Hz, 1H), 8.04 (dd, J = 8.1, 2.0 Hz, 1H), 7.60 (d, J = 8.1 Hz, 1H), 5.36 (s, 1H), 3.35 (s, 6H);

^{13}C NMR (151 MHz, DMSO-d_6): δ 165.8, 156.9, 154.0, 149.2, 138.0, 137.02, 136.97, 131.9, 130.1, 126.8, 122.5, 120.9, 104.3, 54.0;

m.p.: decomp. at 220 °C;

Elemental analysis: calcd for $C_{15}H_{14.6}N_2O_{7.3}$ (**8**·0.3H_2O); H, 4.33; C, 53.04; N, 8.25. found H, 4.04; C, 52.85; N, 8.06.

Scheme S5. Synthesis of **10**

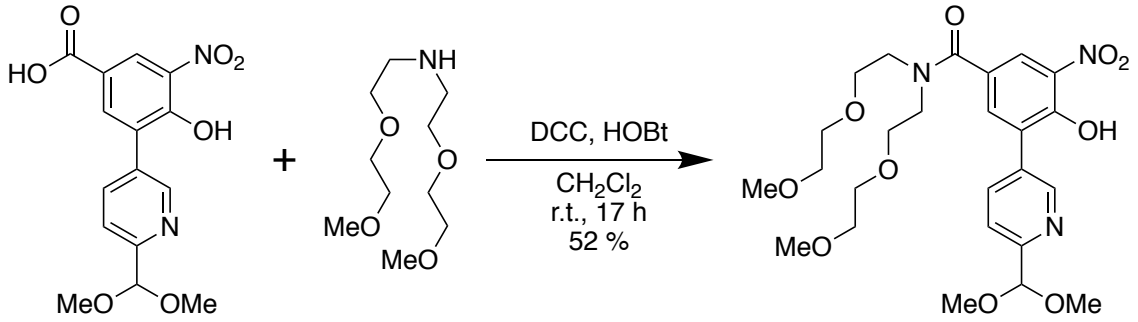

8 **9** **10**

To a mixture of **8** (331.8 mg, 0.993 mmol, 1.0 eq.), DCC (306.2 mg, 1.484 mmol, 1.5 eq.), and 1-hydroxybenzotriazole (154.9 mg, 1.011 mmol. 1.0 eq.) in CH_2Cl_2 (3.5 mL) was added **9**[S10] (450.4 mg, 2.035 mmol, 2.1 eq) and stirred at r.t. for 17 h. The reaction mixture was filtered, and the filtrate was concentrated in vacuo. The residue was purified by column chromatography on silica gel (CH_2Cl_2/MeOH/AcOH = 100/1/1–100/5/1) and GPC to give **10** as a yellow oil (279.6 mg, 0.520 mmol, 52 %).

^{1}H NMR (600 MHz, $CDCl_3$): δ 11.23 (br, 1H), 8.81 (d, J = 2.0 Hz, 1H), 8.41 (d, J = 2.1 Hz, 1H), 8.00 (dd, J = 8.1, 2.0 Hz, 1H), 7.85 (d, J = 2.1 Hz, 1H), 7.66 (d, J = 8.1 Hz, 1H), 5.44 (s, 1H), 3.77–3.52 (16H), 3.45 (s, 6H), 3.41–3.25 (6H);

^{13}C NMR (151 MHz, $CDCl_3$): δ 169.3, 156.9, 153.1, 149.1, 137.40, 137.27, 133.5, 130.9, 129.3, 128.9, 124.5, 120.7, 103.7, 71.8, 70.4, 69.0, 68.1, 58.9, 53.7, 50.2, 45.1;

HRMS (ESI): *m/z* calcd for ([**10**·H$^+$]): 538.2401; found: 538.2401.

Scheme S6. Synthesis of **2**

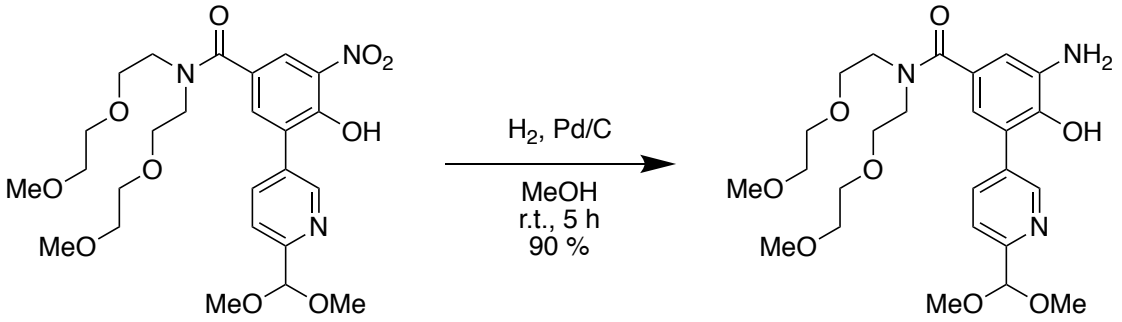

10 **2**

A mixture of **10** (262.2 mg, 487.8 μmol) and Pd 5% /C (155.6 mg) in MeOH (65 mL) was stirred at r.t. for 5 h under H_2 atmosphere. The reaction mixture was filtered and the filtrate was concentrated in vacuo to give **2** as a pale yellow oil (223.8 mg, 441.2 μmol, 90%).
^{1}H NMR (600 MHz, $CDCl_3$): δ 8.67 (d, J = 1.9 Hz, 1H), 7.83 (dd, J = 8.1, 1.9 Hz, 1H), 7.46 (d, J = 8.1 Hz, 1H), 6.79 (d, J = 1.9 Hz, 1H), 6.65 (d, J = 1.9 Hz, 1H), 5.24 (s, 1H), 3.68–3.50 (16H), 3.34 (s, 6H), 3.32 (br, 6H).
^{13}C NMR (151 MHz, $CDCl_3$): δ 172.8, 155.0, 149.2, 142.6, 137.50, 137.45, 134.2, 129.1, 125.9, 120.8, 118.4, 114.7, 103.6, 71.9, 70.3, 69.1, 58.9, 53.7, 49.9, 45.5;
HRMS (ESI): *m/z* calcd for ([**2**·H^+]): 508.2659; found: 508.2663.

Scheme S7. Synthesis of H_6**1**

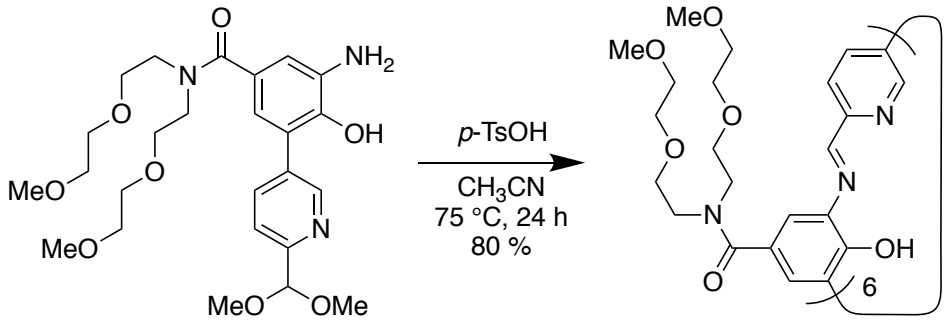

2 H_6**1**

A mixture of **2** (225.1 mg, 443.7 μmol, 1.0 eq.) and *p*-TsOH·H_2O (27.7 mg, 146 μmol, 0.3 eq.) in MeCN (23 mL) was stirred at 75 °C for 24 h. The reaction mixture was added to triethylamine (150 mL). The supernatant was removed by decantation and the precipitate was washed with triethylamine (100 mL × 3) and Et_2O (100 mL × 4). The residue was dried in vacuo to give H_6**1** as a brown solid (157.3 mg, 59.1 μmol, 80%).

^{1}H NMR (600 MHz, $CDCl_3$): δ 8.97 (d, *J* = 1.6 Hz, 1H), 8.96 (s, 1H), 8.45 (dd, *J* = 8.2, 1.6 Hz, 1H), 8.31 (d, *J* = 8.2 Hz, 1H), 7.73 (d, *J* = 1.4 Hz, 1H), 7.67 (d, *J* = 1.4 Hz, 1H), 3.85–3.50 (16H), 3.40–3.30 (6H);

m.p.: decomp. at 250 °C.;

MS (MALDI): *m/z* calcd for ([H_6**1**·Na^+]): 2682.2; found: 2682.1;

Elemental analysis: calcd for $C_{138}H_{180}N_{18}O_{39}$ (H_6**1**·$3H_2O$); H, 6.68; C, 61.05; N, 9.29. found: H, 6.41; C, 61.08; N, 9.20;

IR (KBr): 3338 (br), 3063 (w), 2876 (m), 1625 (s), 1455 (m), 1424 (m), 1359 (m), 1315 (m), 1254 (w), 1228 (w), 1200 (w), 1101 (s), 1026 (w), 962 (w), 889 (w), 848 (w), 766 (w), 646 (w), 564 (w), 472 (w), 445 cm^{-1};

UV/Vis ($CHCl_3$): λ_{max} 392 nm.

Scheme S8. Synthesis of [**1**Pd$_6$L$_6$](BF$_4$)$_6$

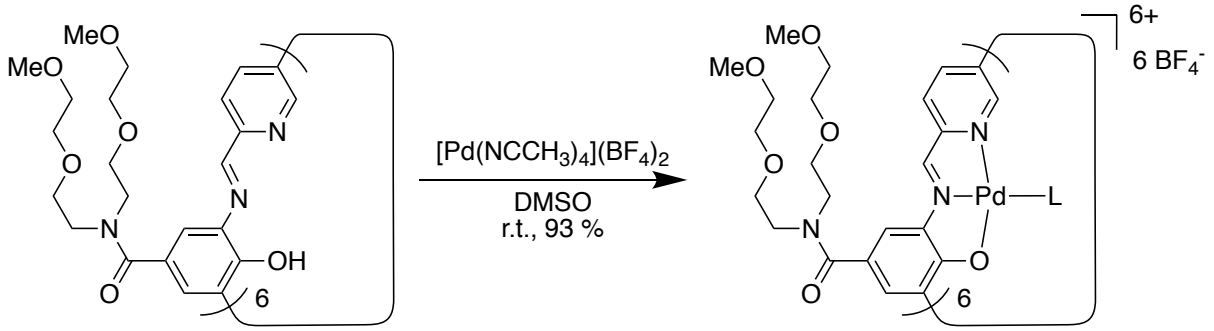

H$_6$**1** [**1**Pd$_6$L$_6$](BF$_4$)$_6$

To a solution of H$_6$**1** (149.5 mg, 56.2 μmol, 1.0 eq.) in DMSO (15 mL) was added a solution of [Pd(NCMe)$_4$](BF$_4$)$_2$ (156.1 mg, 351.4 μmol, 6.3 eq.) in DMSO (5 mL). The solvent was removed in vacuo. To the residue was added MeCN (15 mL), and the solution was added to Et$_2$O (70 mL). The supernatant was removed by decantation and the precipitate was washed with MeCN/Et$_2$O (15mL/70 mL × 3) and Et$_2$O (100 mL × 4). To the residue was added MeCN (17 mL), and the solution was added Et$_2$O (120 mL). The supernatant was removed by decantation and the precipitate was washed with Et$_2$O (50 mL × 3). The residue was dried in vacuo to give [**1**Pd$_6$](BF$_4$)$_6$·4MeCN·6H$_2$O·0.25Et$_2$O as a purple solid (214.1 mg, 52.2 μmol, 93%).

m.p. >250 °C;

Elemental analysis: calcd for $C_{147}H_{194.5}N_{22}O_{42.25}Pd_6B_6F_{24}$ ([**1**Pd$_6$](BF$_4$)$_6$·4MeCN·6H$_2$O·0.25Et$_2$O); H, 4.78; C, 43.01; N, 7.51, found: H, 4.51; C, 42.82; N, 7.43;

^{1}H NMR (600 MHz, CD$_3$CN): δ 8.51 (br, 1H), 8.25 (dd, *J* = 8.1, 1.7 Hz, 1H), 8.20 (s, 1H), 7.89 (d, *J* = 8.1 Hz, 1H), 7.74 (d, *J* = 1.7 Hz, 1H), 7.53 (d, *J* = 1.7 Hz, 1H), 3.65–3.50 (m, 16H), 3.29 (s, 6H);

^{11}B NMR (193 MHz, CD$_3$CN): δ –1.2;

^{19}F NMR (565 MHz, CD$_3$CN): δ –150.9;

ESI-TOF MS *m*/*z* [**1**Pd$_6$]$^{6+}$ calcd for $C_{138}H_{168}N_{18}O_{36}Pd_6$: 548.7695. found: 548.7684; [**1**Pd$_6$(NCMe)$_6$]$^{6+}$ calcd for $C_{150}H_{186}N_{24}O_{36}Pd_6$: 589.7961. found: 589.7941;

IR (KBr): 3409 (br), 3054 (w), 2879 (m), 1599 (s), 1475 (m), 1448 (s), 1387 (w), 1356 (m), 1295 (s), 1230 (s), 1090 (s), 918 (w), 847 (w), 765 (w), 741 (w), 710 (w), 637 (w), 604 (w), 574 (w), 521 (w), 472 (w), 426 (w) cm^{-1}.

UV/Vis (MeCN): λ_{max} 572 nm

Scheme S9. Synthesis of [**1**$Zn_6(acac)_6$]

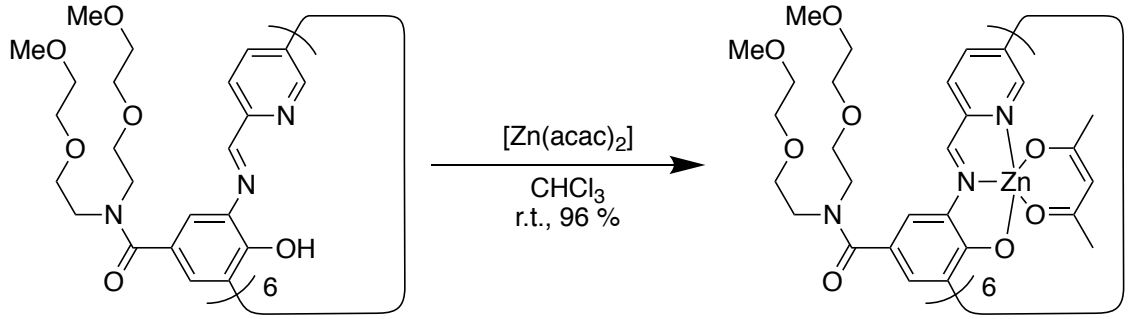

H_6**1** [**1**$Zn_6(acac)_6$]

To H_6**1** (27.3 mg, 10 μmol, 1.0 eq.) were added a solution of [$Zn(acac)_2$] (15.8 mg, 60 μmol, 6.0 eq.) in $CHCl_3$ (2 mL) and additional $CHCl_3$ (2 mL). The solvent was removed in vacuo. The residue was dried in vacuo to give [**1**$Zn_6(acac)_6$] as a red solid (35.2 mg, 9.69 μmol, 96%).

m.p. >250 °C;

Elemental analysis: calcd for $C_{170}H_{212}N_{18}O_{48}Cl_6Zn_6$ (**1**Zn_6·$2CHCl_3$); H, 5.51; C, 52.62; N, 6.50. found: H, 5.77; C, 52.55; N, 6.19;

^{1}H NMR (600 MHz, $CDCl_3$): δ 9.56 (d, J = 1.4 Hz, 1H), 8.79 (s, 1H), 8.01 (d, J = 1.6 Hz, 1H), 8.00 (dd, J = 8.2, 1.4 Hz, 1H), 7.67 (d, J = 8.2 Hz, 1H), 7.57 (d, J = 1.6 Hz, 1H), 5.60 (s, 1H), 3.78–3.75 (8H), 3.67 (m, 4H), 3.57 (m, 4H), 3.36 (s, 6H), 2.08 (s, 6H);

^{13}C NMR (151 MHz, $CDCl_3$): δ 194.0, 172.1, 166.3, 151.8, 147.5, 145.2, 140.6, 137.6, 132.9, 130.8, 126.4, 125.7, 120.1, 117.9, 100.48, 100.43, 71.9, 70.5, 69.0, 58.9, 28.4;

IR (KBr): 3436 (br), 2874 (m), 1588 (s), 1521 (s), 1393 (s), 1361 (s), 1266 (w), 1199 (w), 1160 (s), 1100 (s), 1017 (s), 925 (w), 848 (w), 766 (w), 652 (w), 575 (w), 418 (w), 407 (w), cm^{-1};

UV/Vis ($CHCl_3$/CH_3OH = 10:1 (v/v)): λ_{max} 527 nm;

Emission ($CHCl_3$/CH_3OH = 10:1 (v/v)): 671 nm (λ_{ex} = 527 nm); emission quantum yield ($CHCl_3$/CH_3OH = 10:1 (v/v)): Φ_F = 0.019 (λ_{ex} = 527 nm);

Characterization data

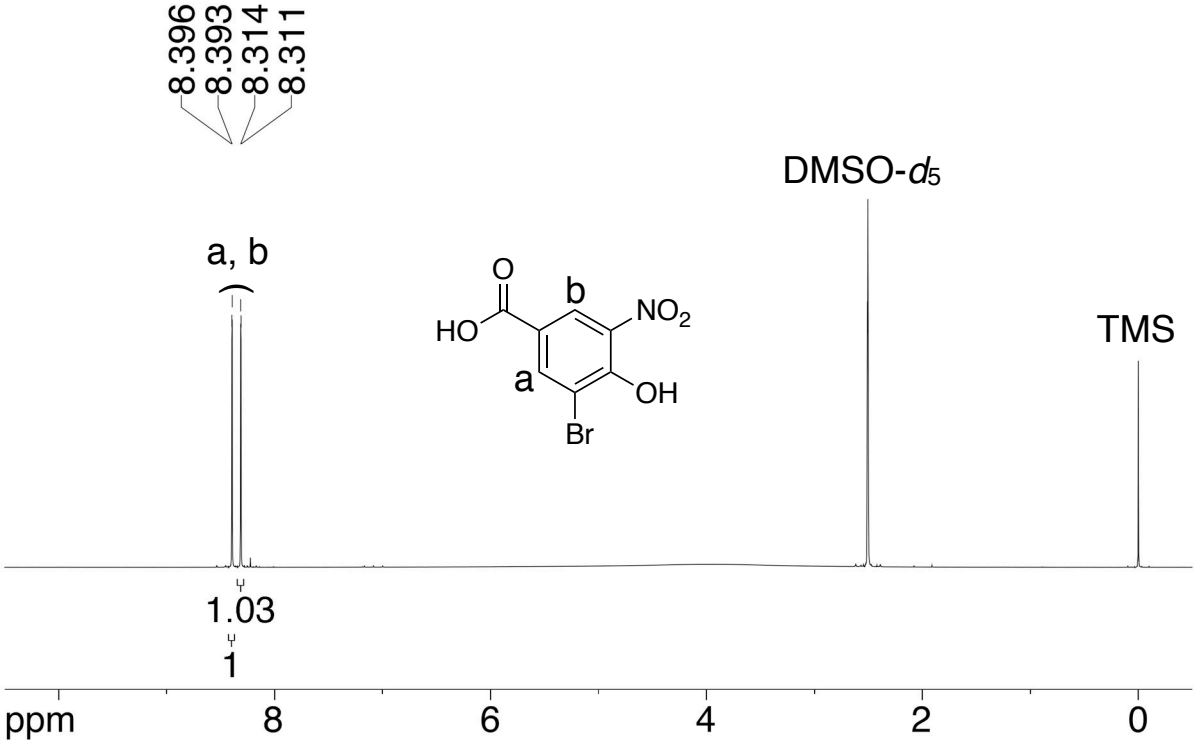

Figure S1. ^{1}H NMR spectrum of **4** (600 MHz, DMSO-d_6).

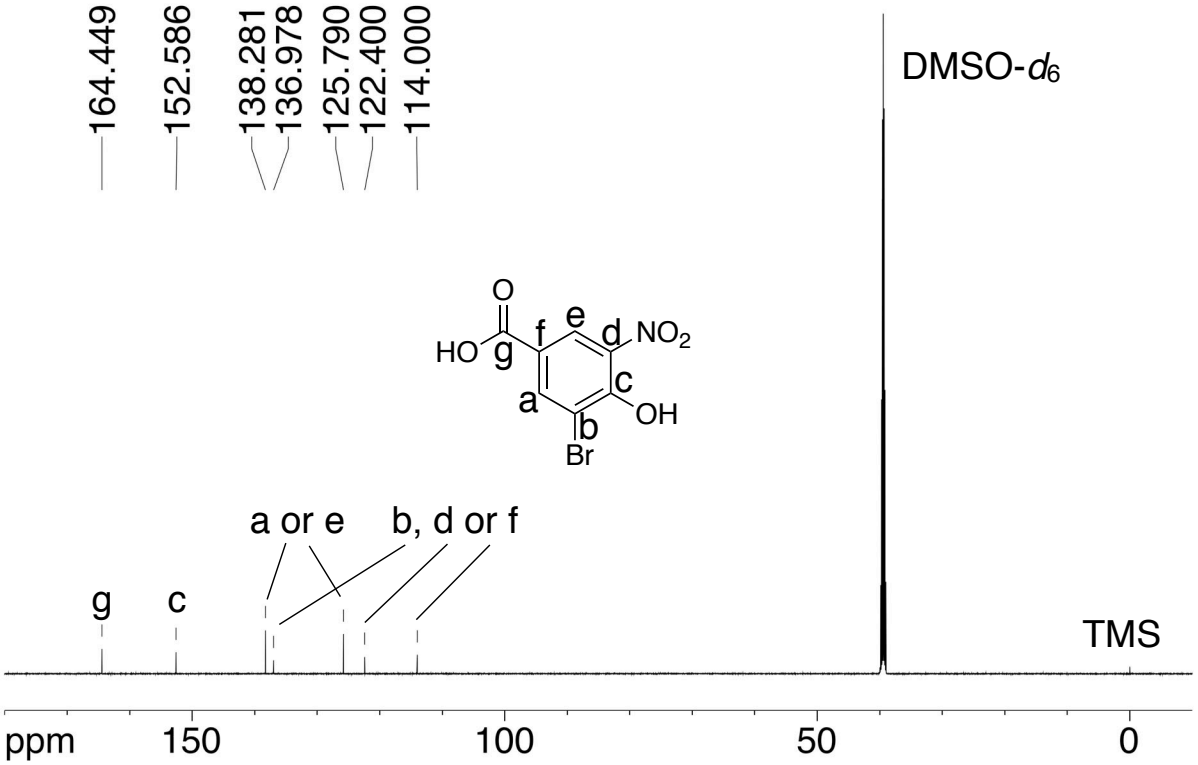

Figure S2. ^{13}C NMR spectrum of **4** (151 MHz, DMSO-d_6).

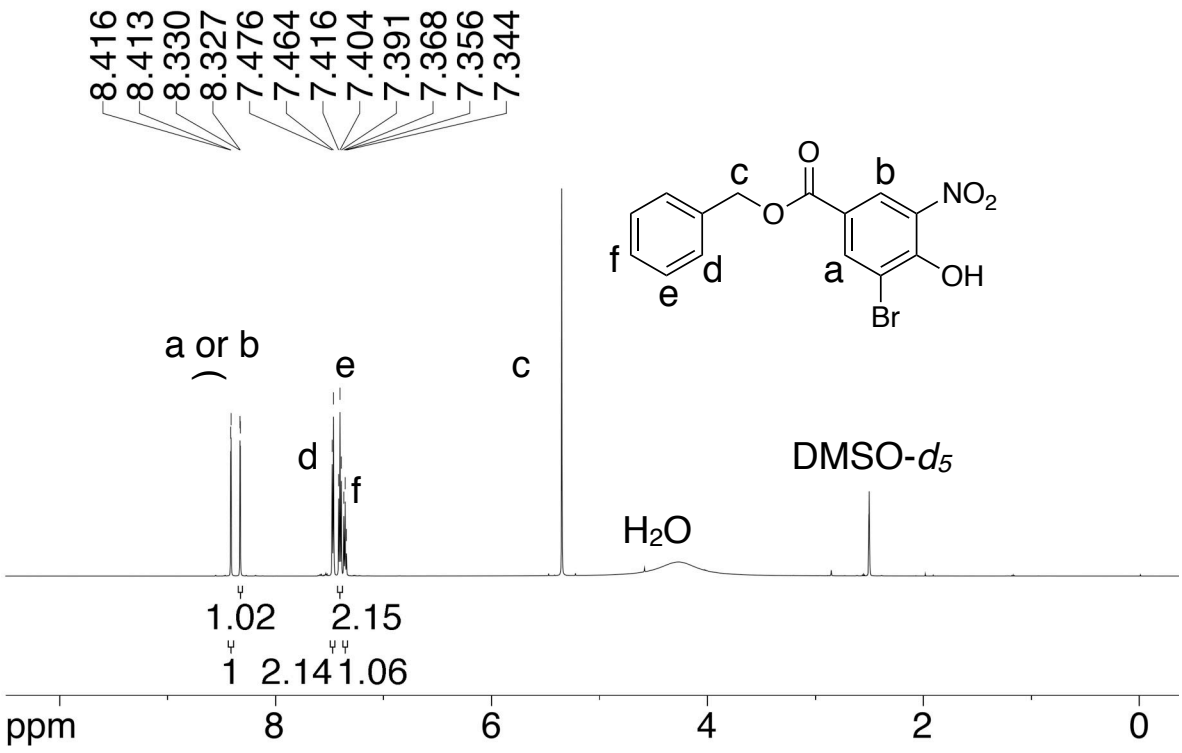

Figure S3. [1]H NMR spectrum of **5** (600 MHz, DMSO-d_6).

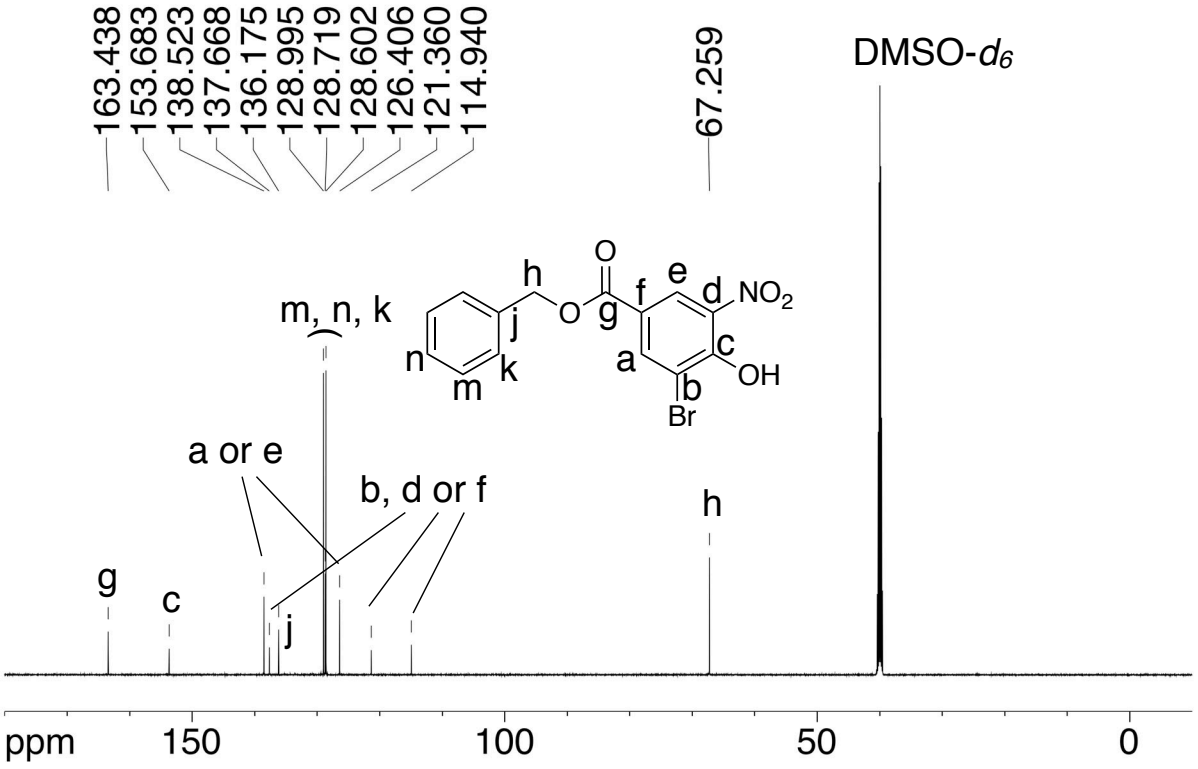

Figure S4. [13]C NMR spectrum of **5** (151 MHz, DMSO-d_6).

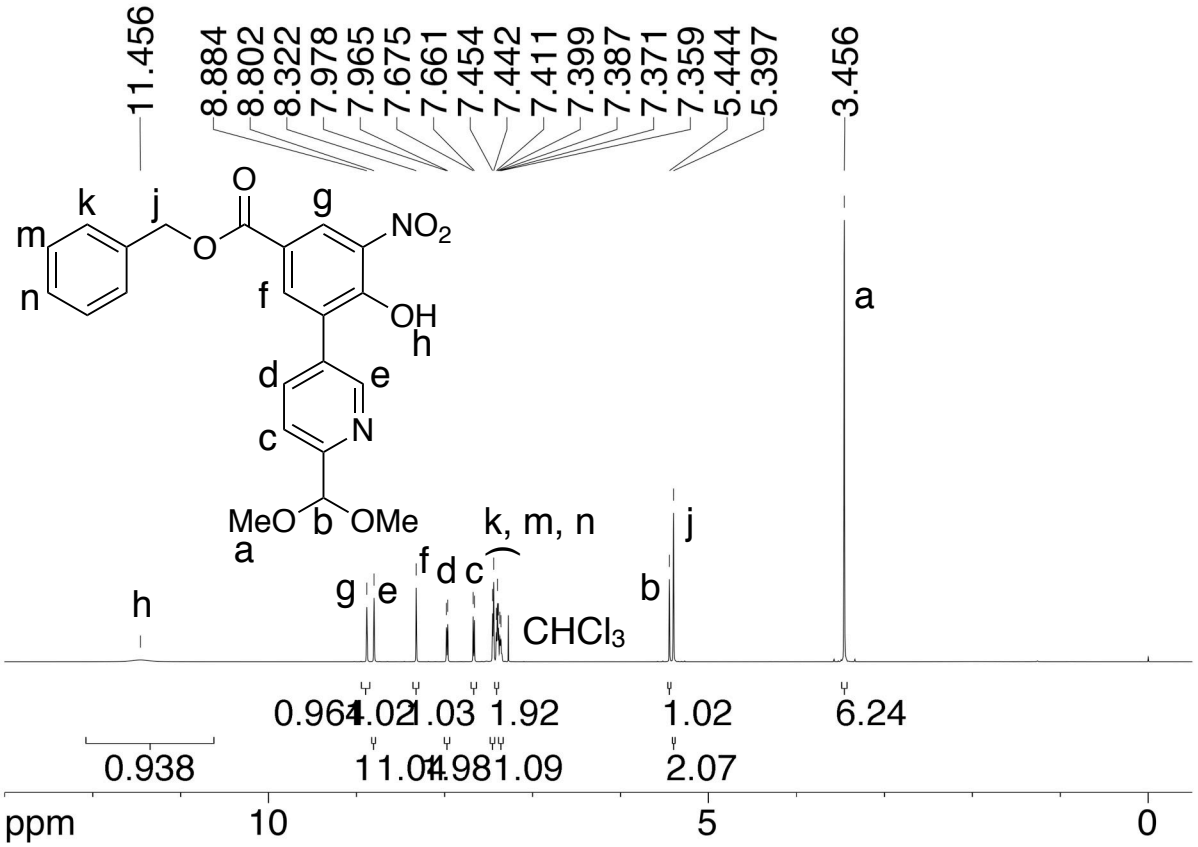

Figure S5. ^{1}H NMR spectrum of **7** (600 MHz, $CDCl_3$).

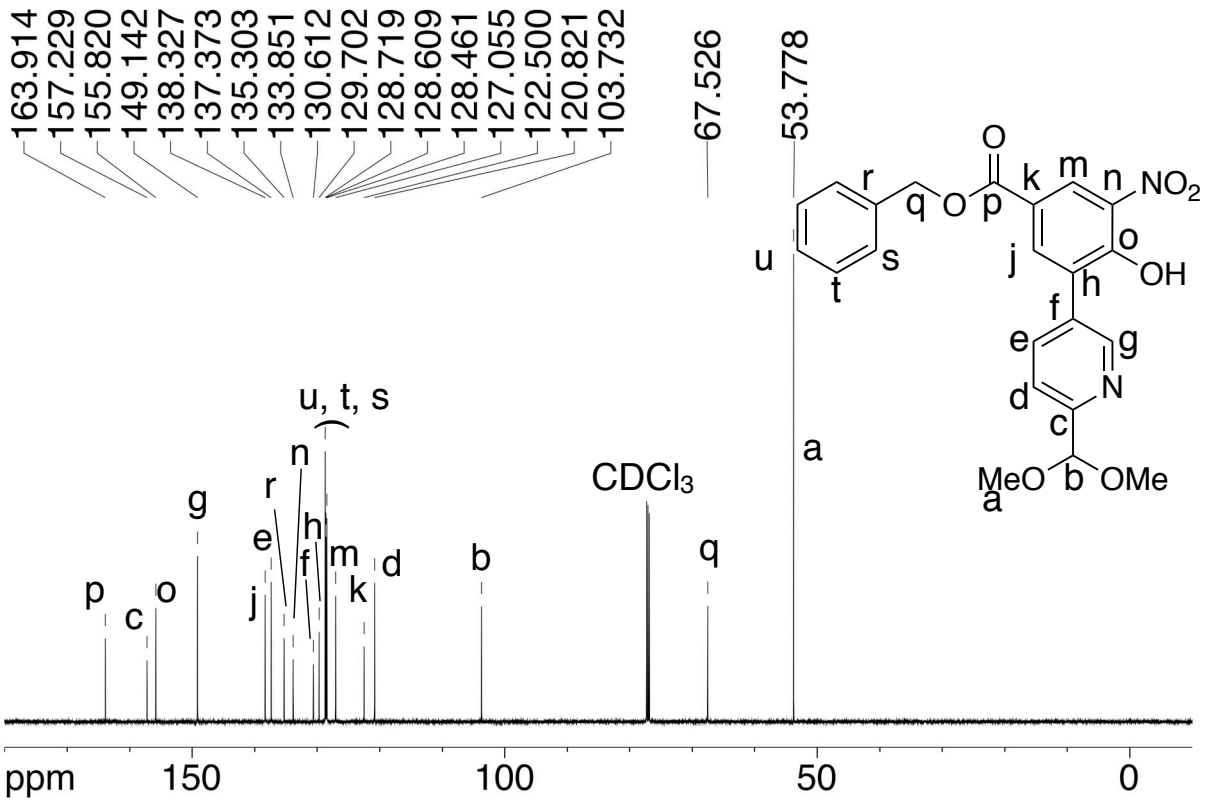

Figure S6. ^{13}C NMR spectrum of **7** (151 MHz, $CDCl_3$).

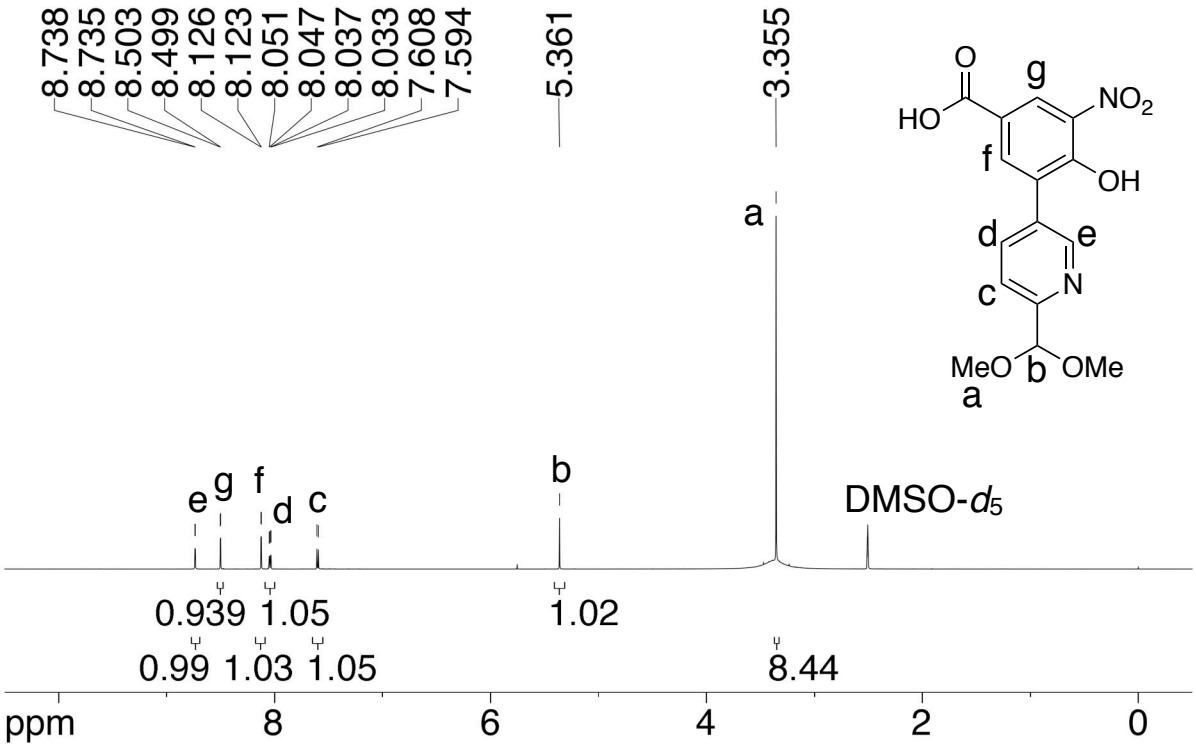

Figure S7. [1]H NMR spectrum of **8** (600 MHz, DMSO-d_6).

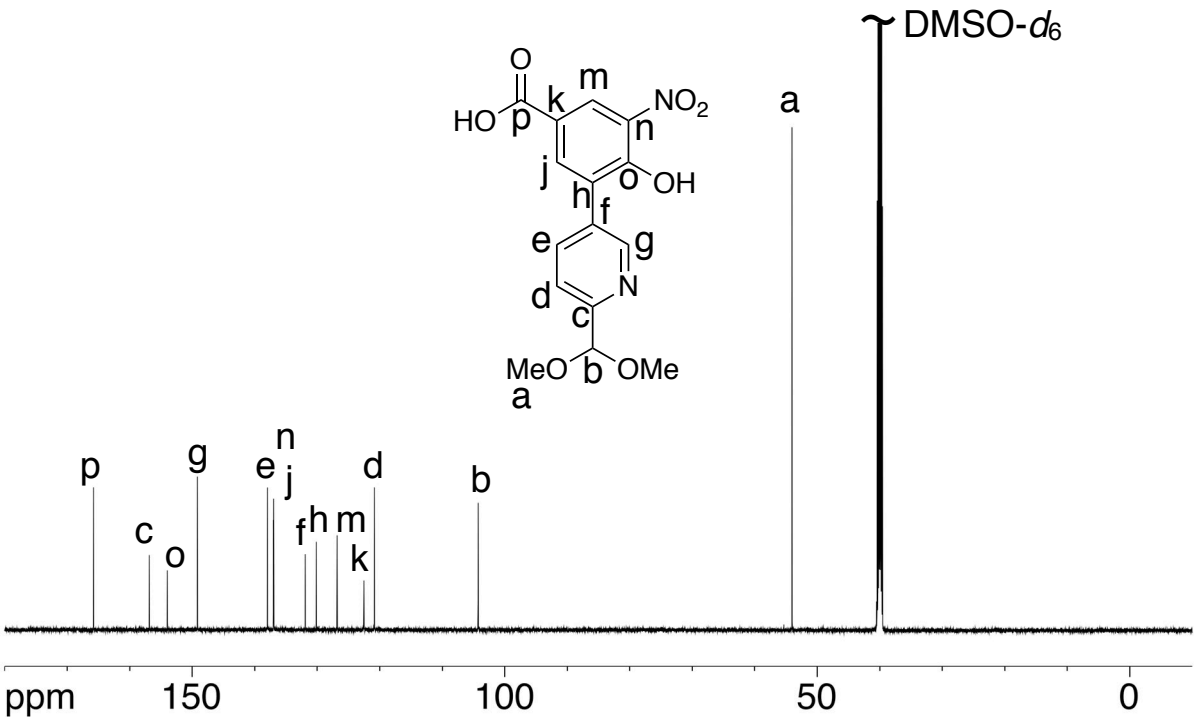

Figure S8. [13]C NMR spectrum of **8** (151 MHz, DMSO-d_6).

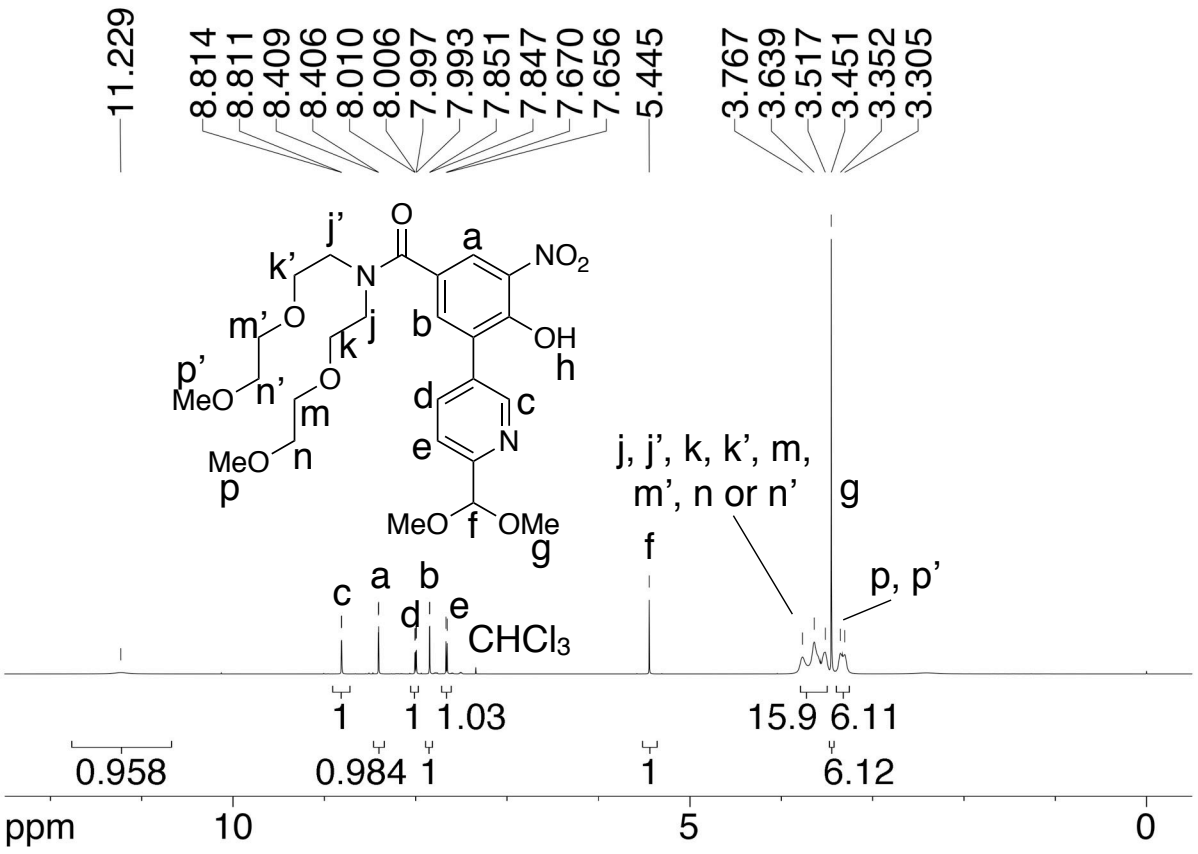

Figure S9. ^{1}H NMR spectrum of **10** (600 MHz, $CDCl_3$).

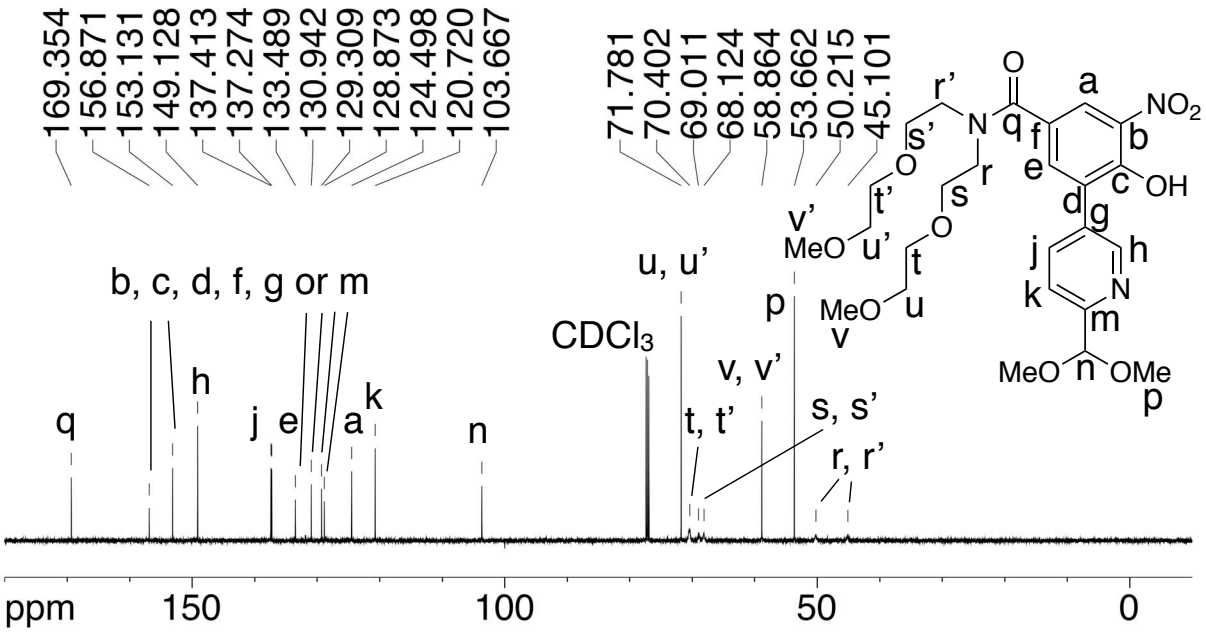

Figure S10. ^{13}C NMR spectrum of **10** (151 MHz, $CDCl_3$).

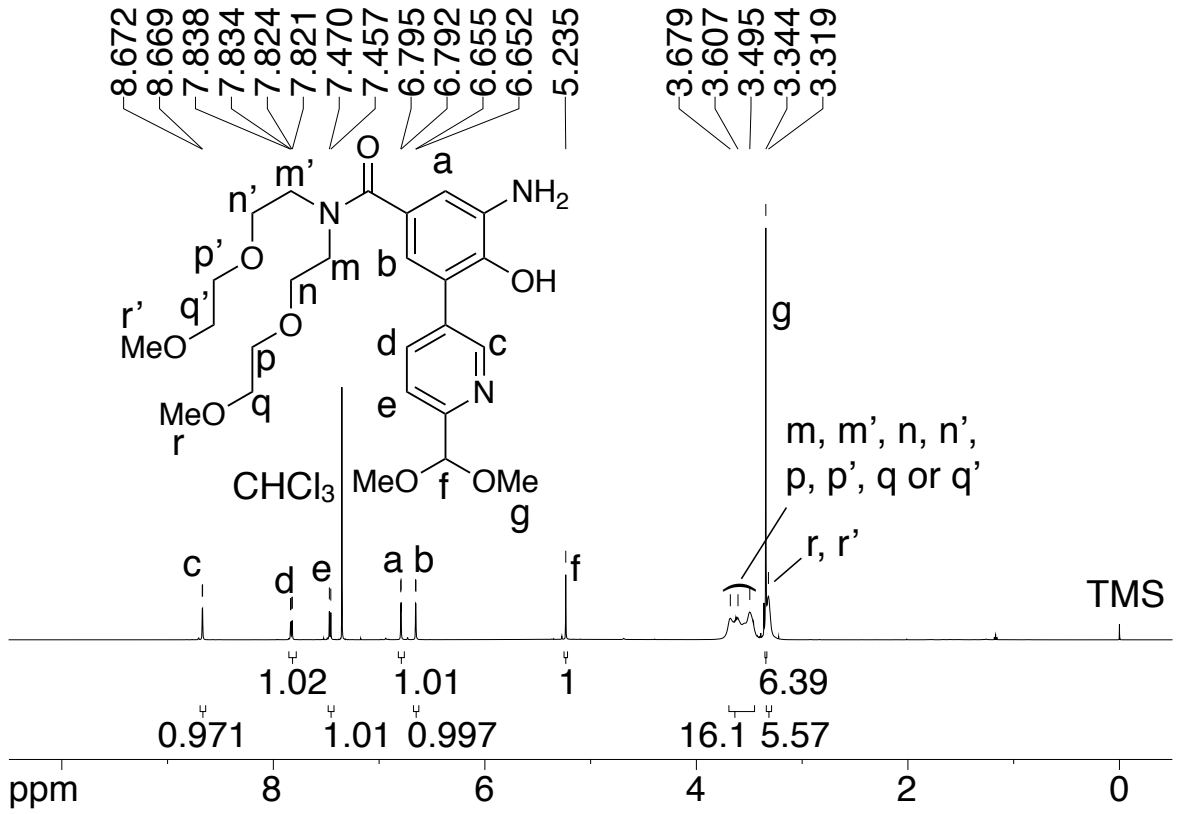

Figure S11. ^{1}H NMR spectrum of **2** (600 MHz, $CDCl_3$).

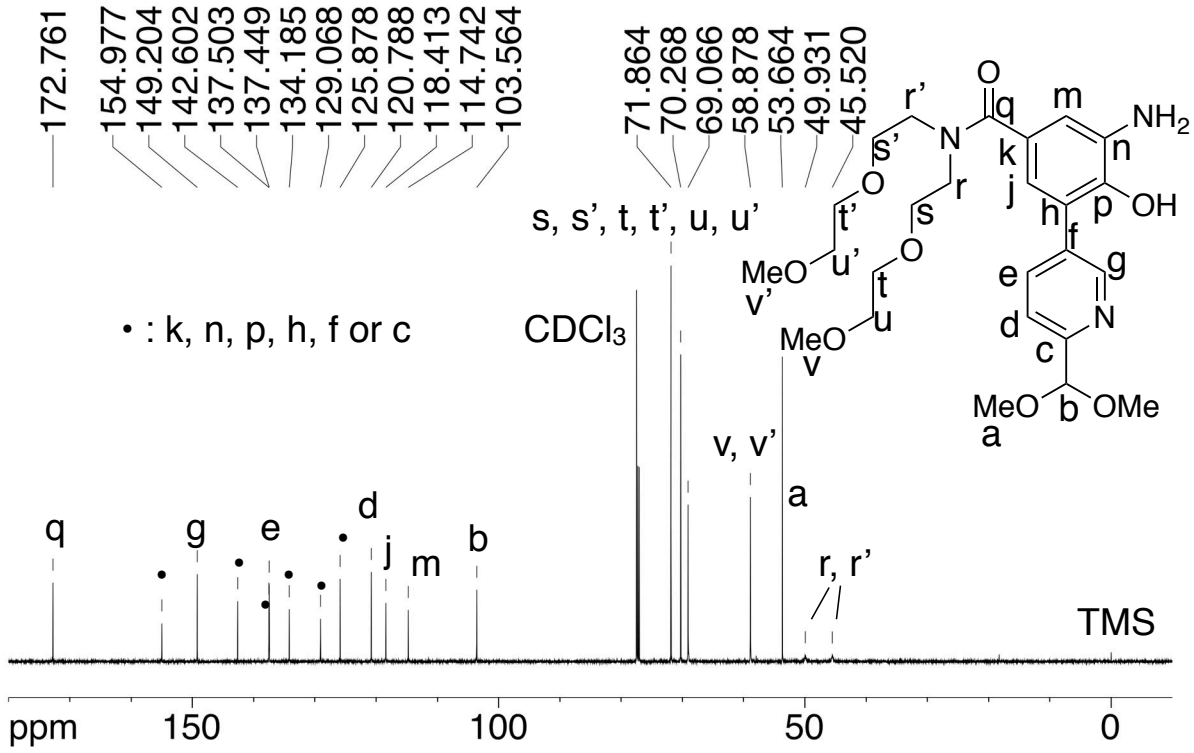

Figure S12. ^{13}C NMR spectrum of **2** (151 MHz, $CDCl_3$).

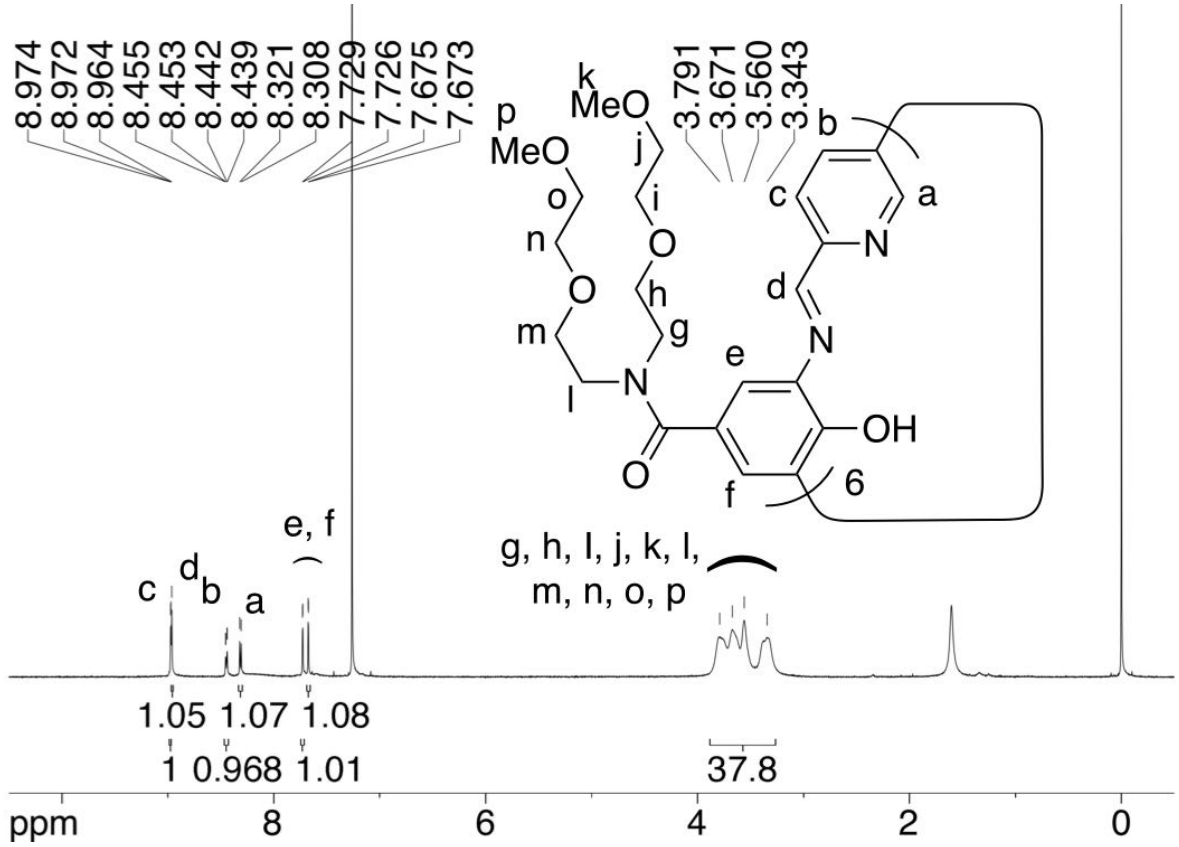

Figure S13. ^{1}H NMR spectrum of H_6**1** (600 MHz, $CDCl_3$).

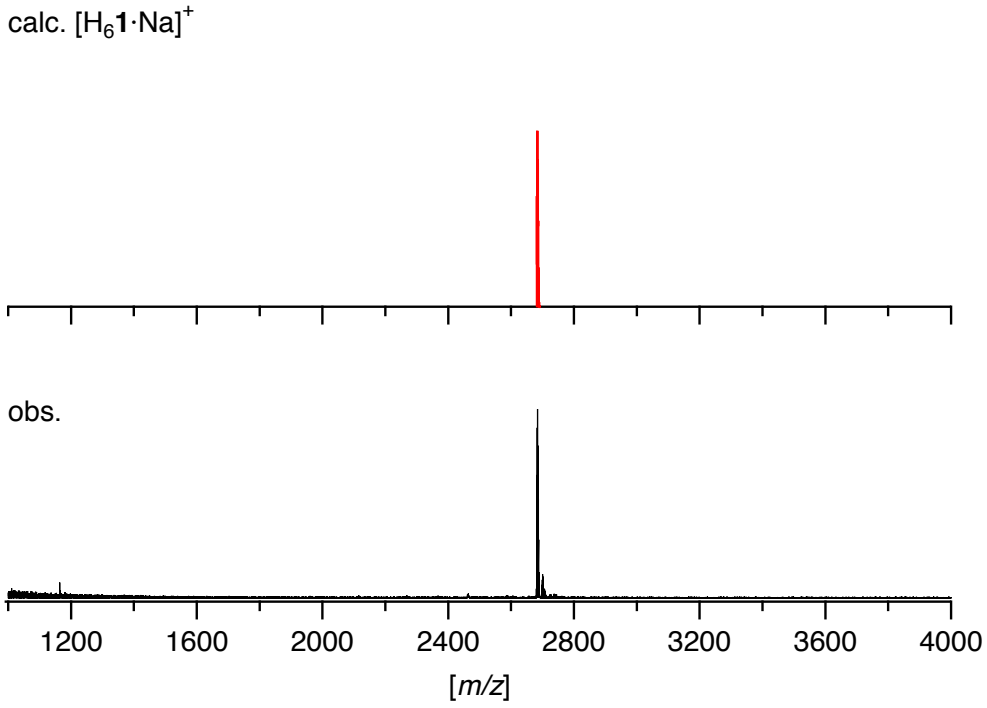

Figure S14. MALDI MS spectrum of H$_6$**1** (*m*/*z* = 1000–4000) (matrix: CHCA, positive).

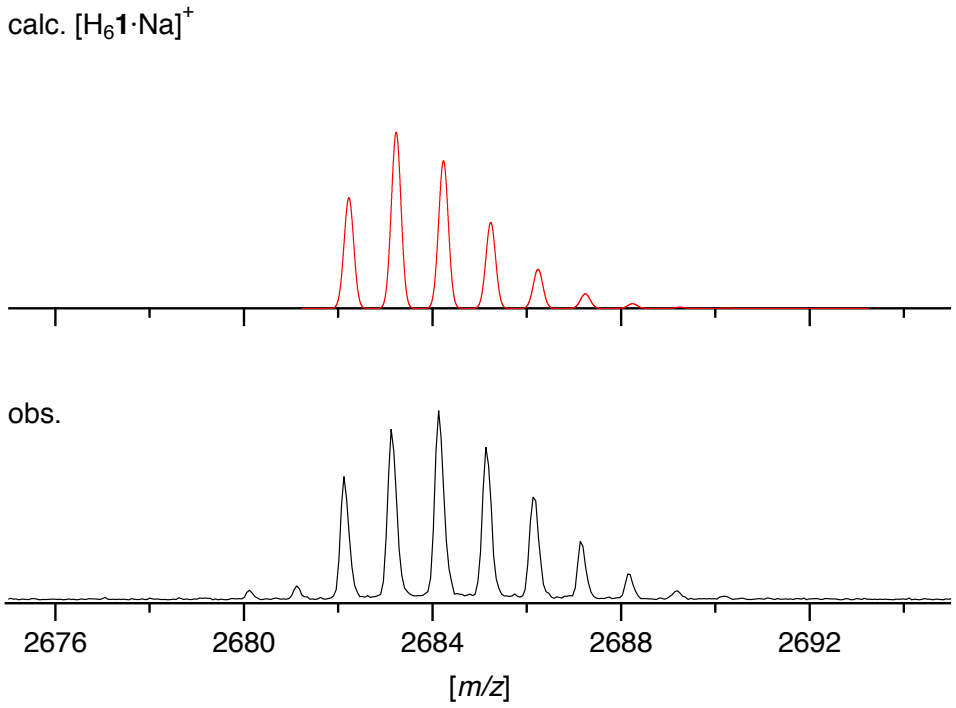

Figure S15. MALDI MS spectrum of H$_6$**1** (*m*/*z* = 2676–2693) (matrix: CHCA, positive).

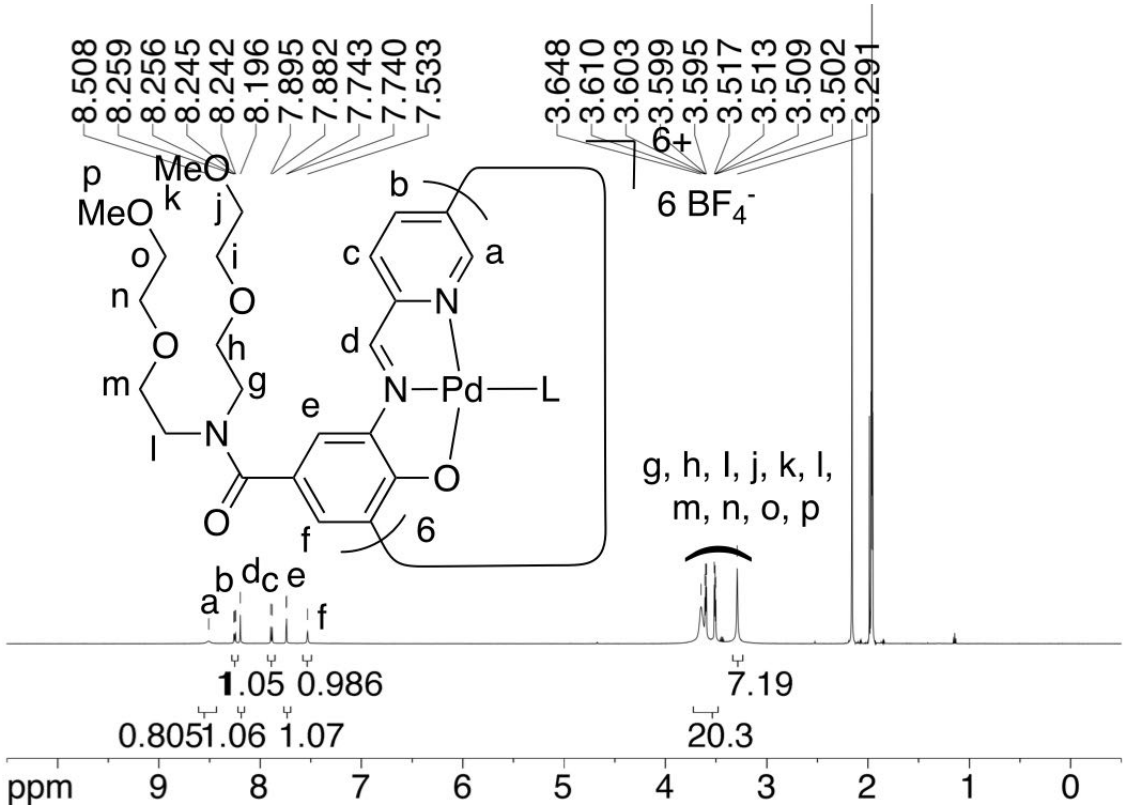

Figure S16. ^{1}H NMR spectrum of [**1**Pd$_6$L$_6$](BF$_4$)$_6$ (600 MHz, CD$_3$CN).

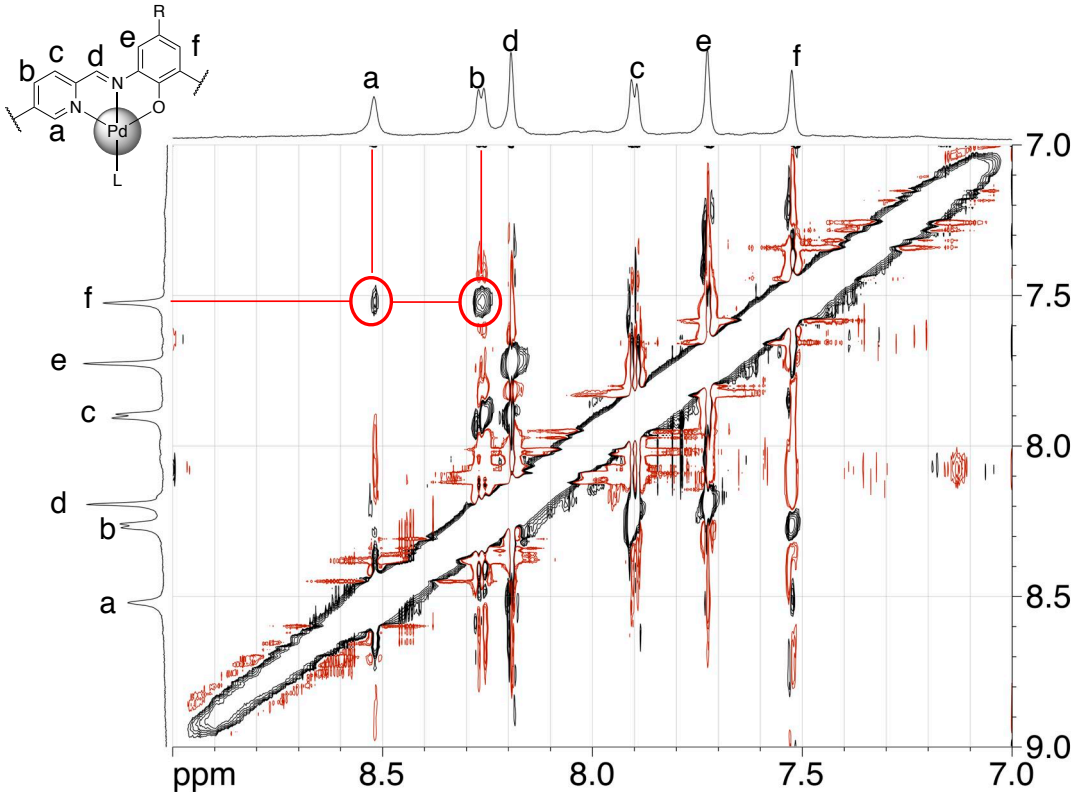

Figure S17. ^{1}H–^{1}H NOESY spectrum of [**1**Pd$_6$L$_6$](BF$_4$)$_6$ (600 MHz, CD$_3$CN, 328 K). The NOE between protons *a* and *f* suggests that Pd complex [**1**Pd$_6$(CD$_3$CN)$_6$](BF$_4$)$_6$ takes a twisted conformation.

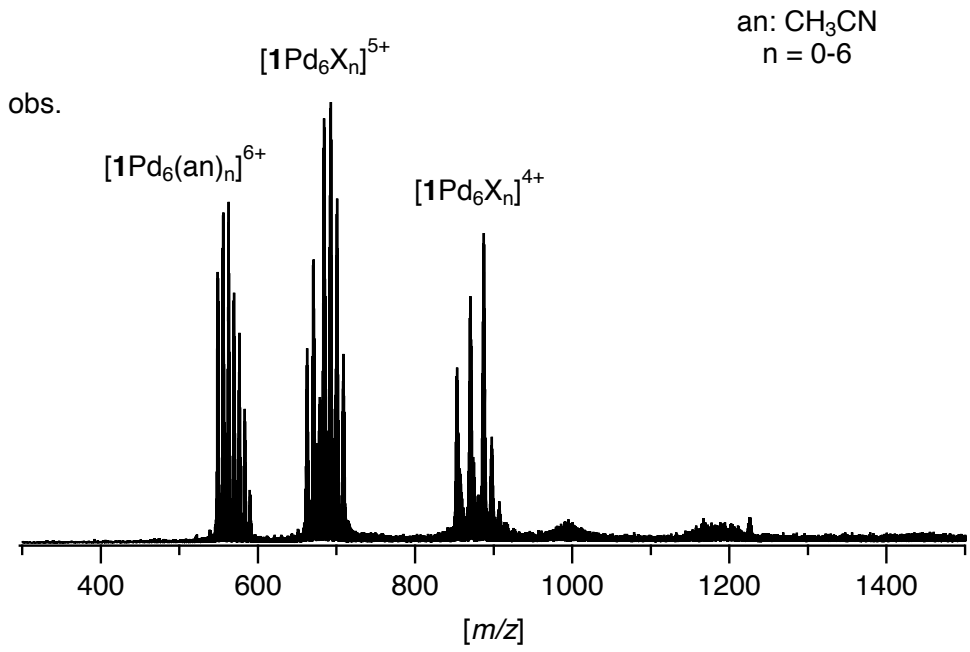

Figure S18. ESI-TOF mass spectrum of $[\mathbf{1}Pd_6L_6](BF_4)_6$. ($m/z$ = 300–1500) (CH_3CN, positive).

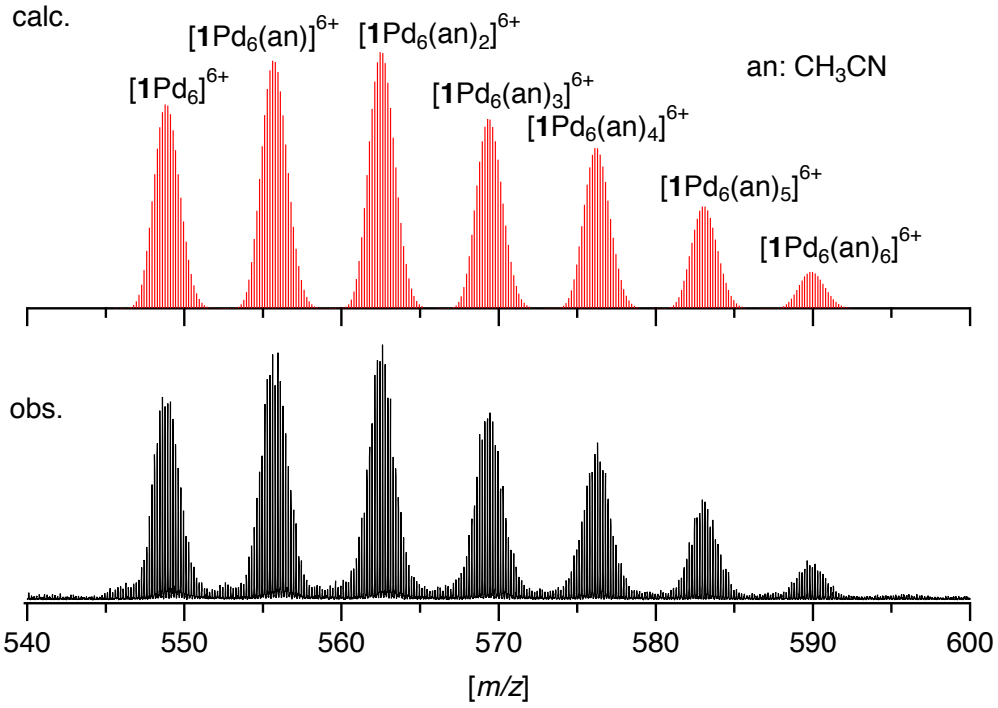

Figure S19. ESI-TOF mass spectrum of $[\mathbf{1}Pd_6L_6](BF_4)_6$ (m/z = 540–600) (CH_3CN, positive).

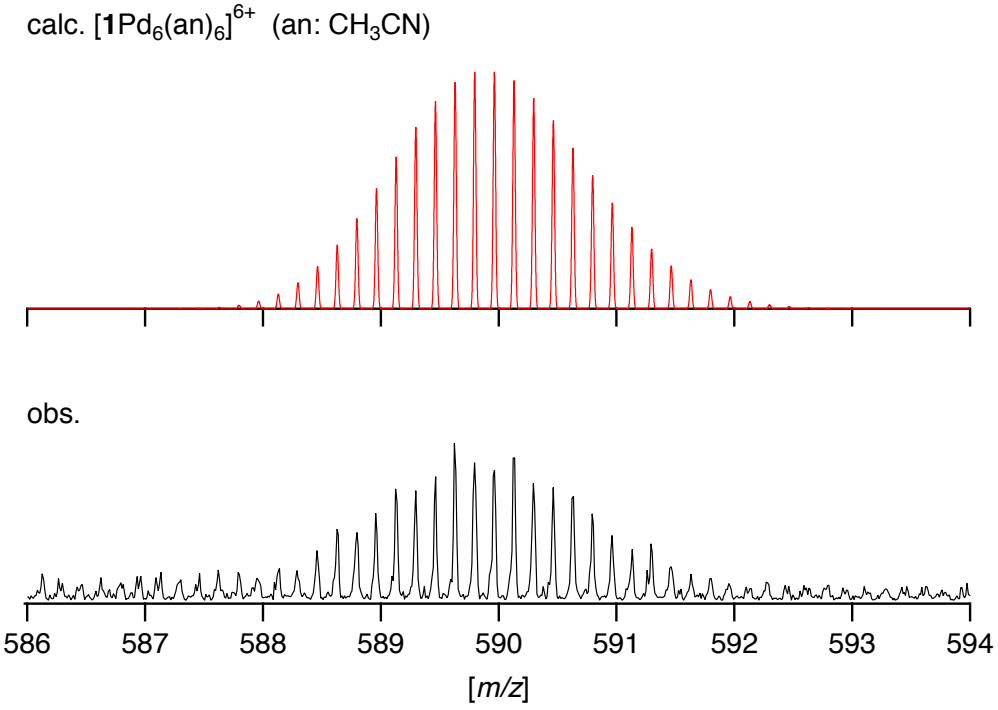

Figure S20. ESI-TOF mass spectrum of [**1**Pd_6L_6]$(BF_4)_6$ (*m*/*z* = 586–594) (CH_3CN, positive).

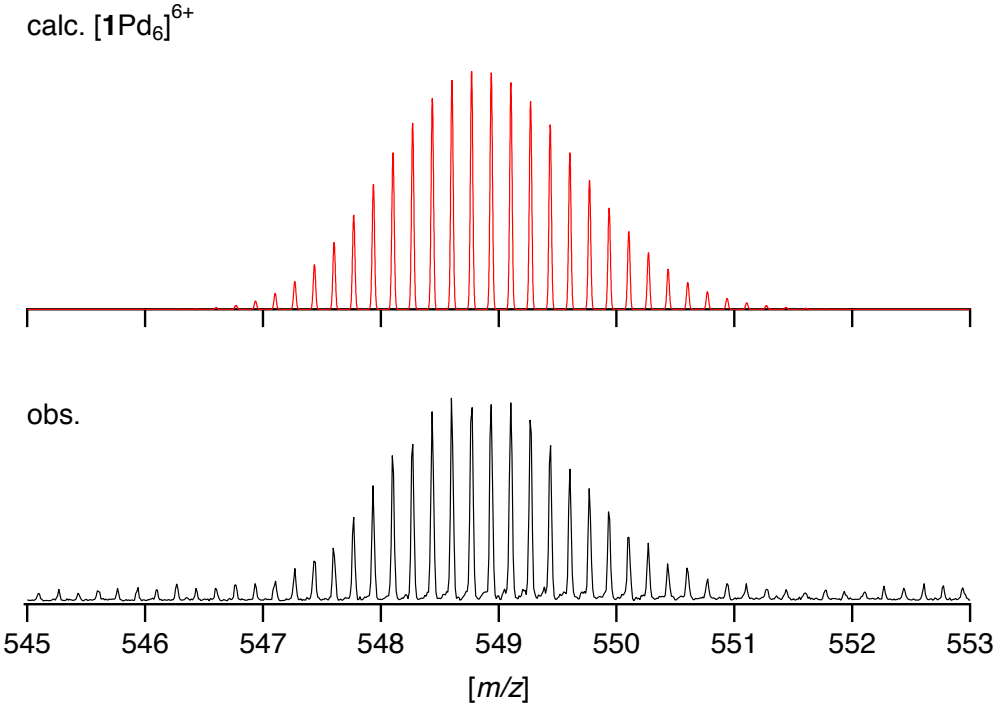

Figure S21. ESI-TOF mass spectrum of [**1**Pd_6L_6]$(BF_4)_6$ (*m*/*z* = 545–553) (CH_3CN, positive).

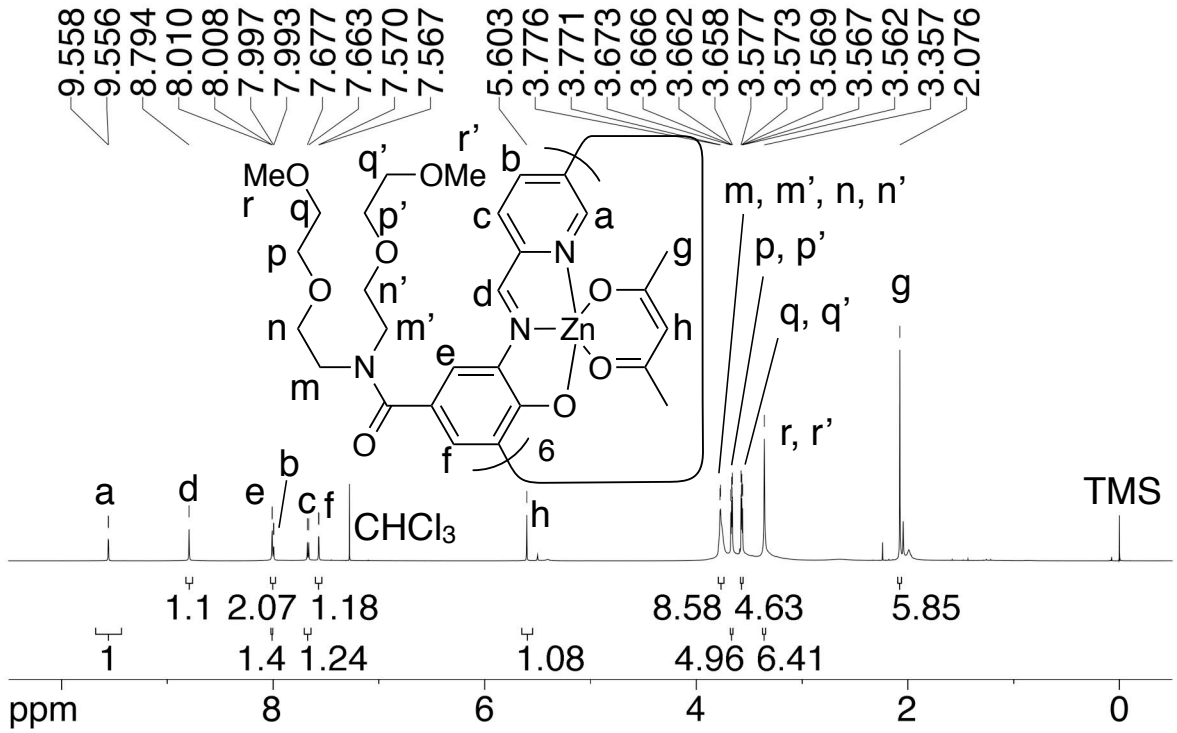

Figure S22. ^{1}H NMR spectrum of [**1**Zn$_6$(acac)$_6$] (600 MHz, $CDCl_3$).

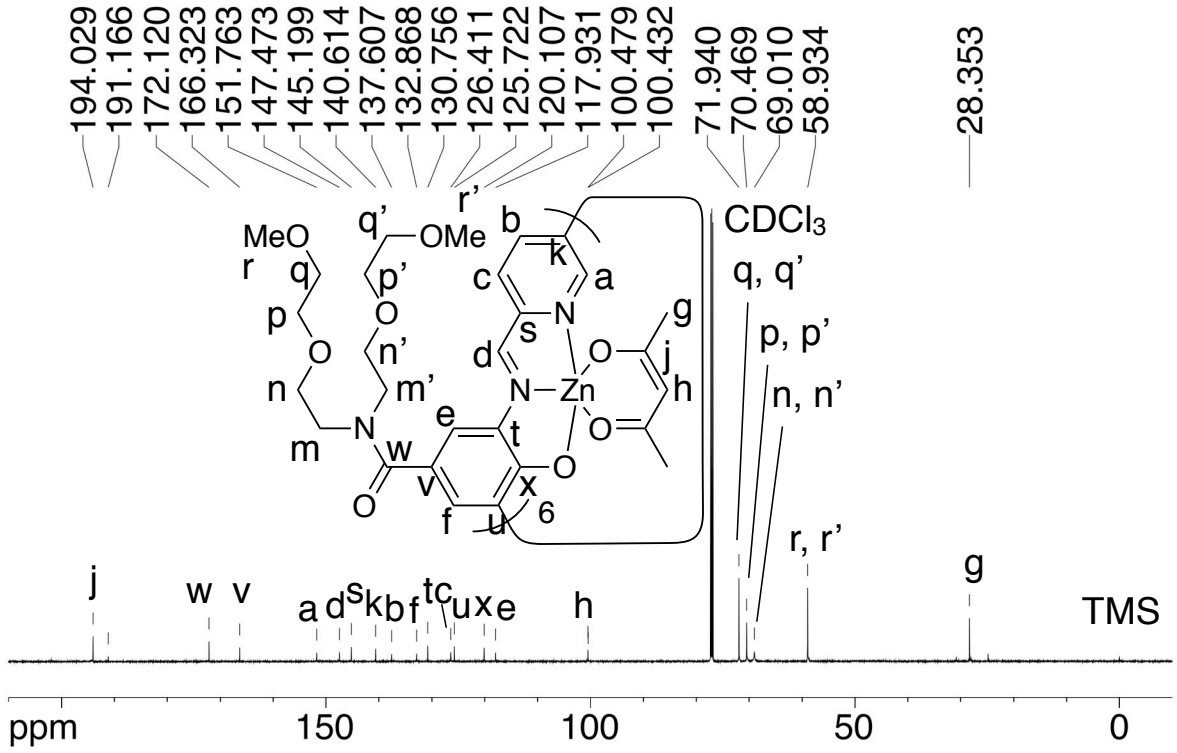

Figure S23. ^{13}C NMR spectrum of [**1**Zn$_6$(acac)$_6$] (151 MHz, $CDCl_3$).

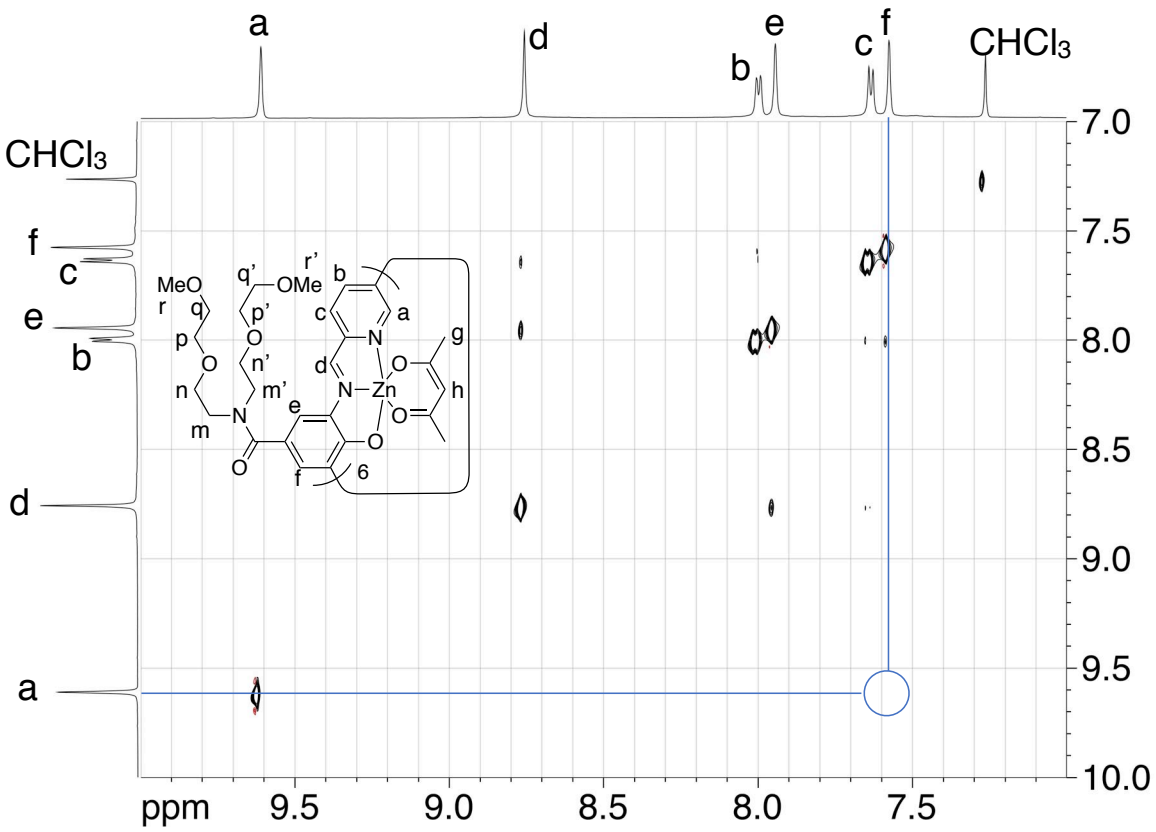

Figure S24. ^{1}H–^{1}H NOESY spectrum of [**1**Zn$_6$(acac)$_6$] (600 MHz, $CDCl_3$, 328 K). Absence of NOE between protons *a* and *f* suggests that Zn complex [**1**Zn$_6$(acac)$_6$] does not take a twisted conformation, which is in contrast to Pd complex [**1**Pd$_6$(CH_3CN)$_6$](BF_4)$_6$.

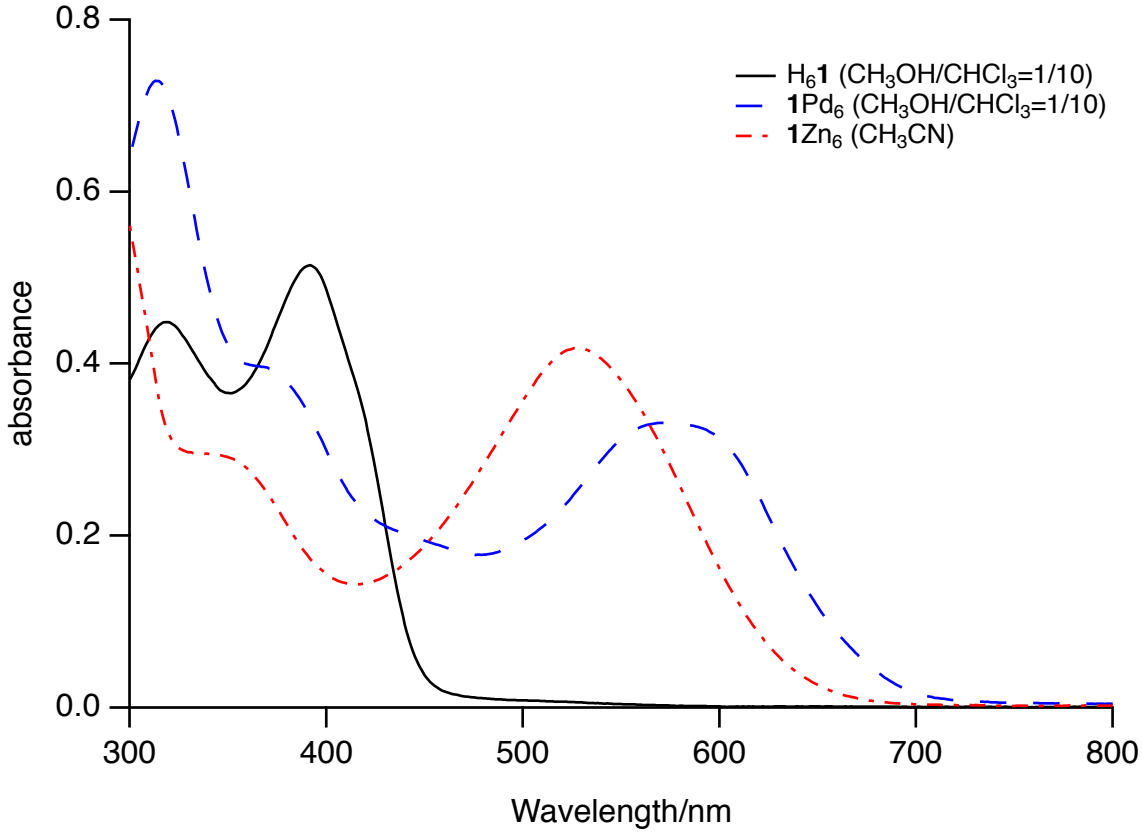

Figure S25. UV-vis absorption spectra of H_6**1** ($CHCl_3/CH_3OH$ = 10:1 (v/v), 4.8 μmol/L, *l* = 1.0 cm), [**1**Pd_6L_6]$(BF_4)_6$ (CH_3CN, 7.1 μmol/L, *l* = 1.0 cm), and [**1**$Zn_6(acac)_6$] ($CHCl_3/CH_3OH$ = 10:1 (v/v), 5.6 μmol/L, *l* = 1.0 cm).

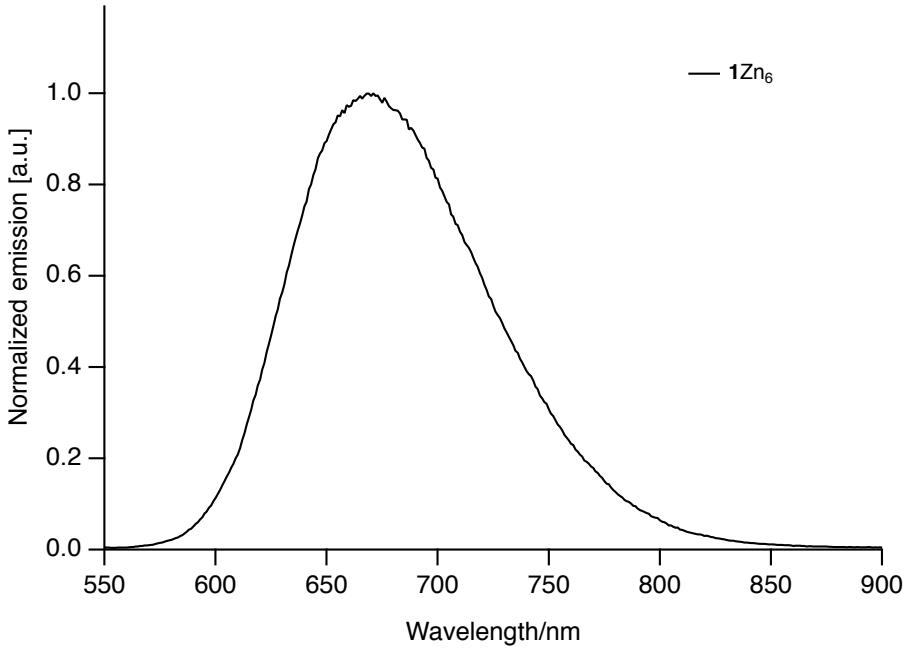

Figure S26. Emission spectrum of [**1**$Zn_6(acac)_6$] ($CHCl_3/CH_3OH$ = 10:1 (v/v), 5.6 μmol/L, *l* = 1.0 cm).

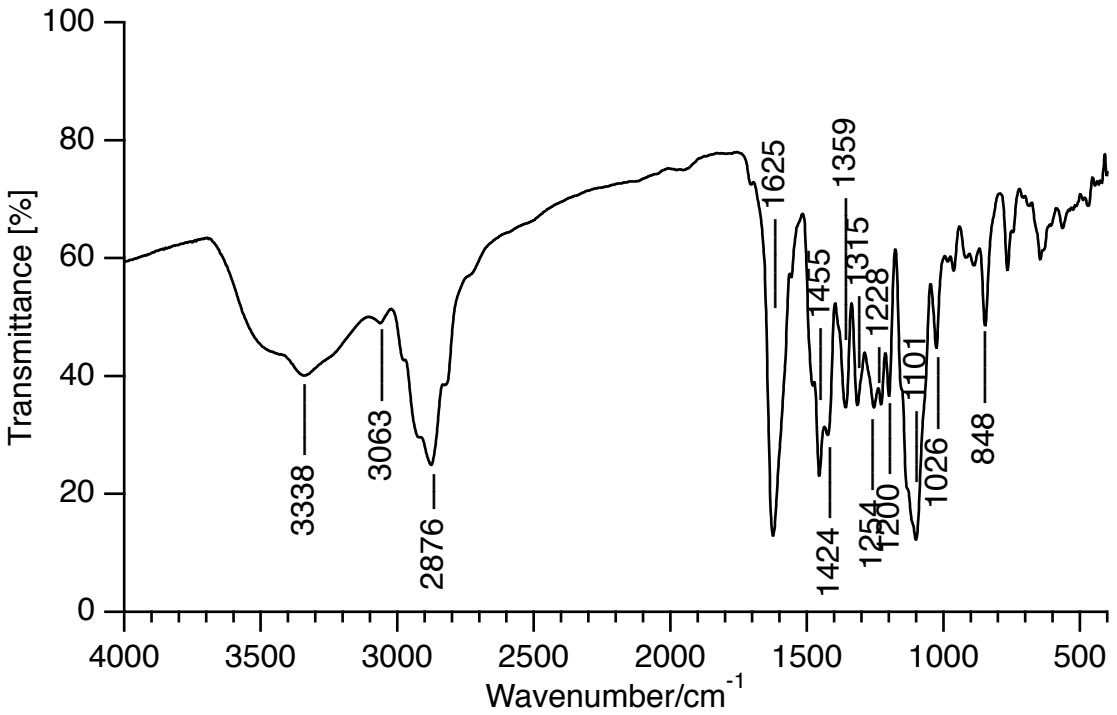

Figure S27. IR spectrum of H_6**1** (KBr).

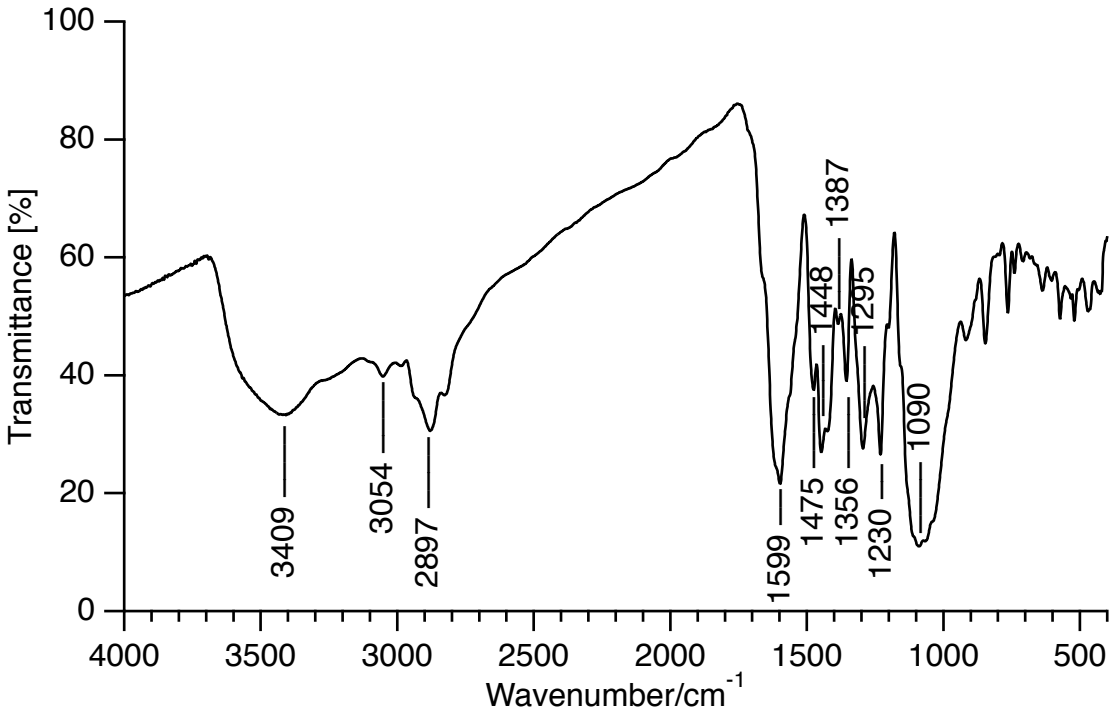

Figure S28. IR spectrum of[**1**Pd_6L_6]$(BF_4)_6$ (KBr).

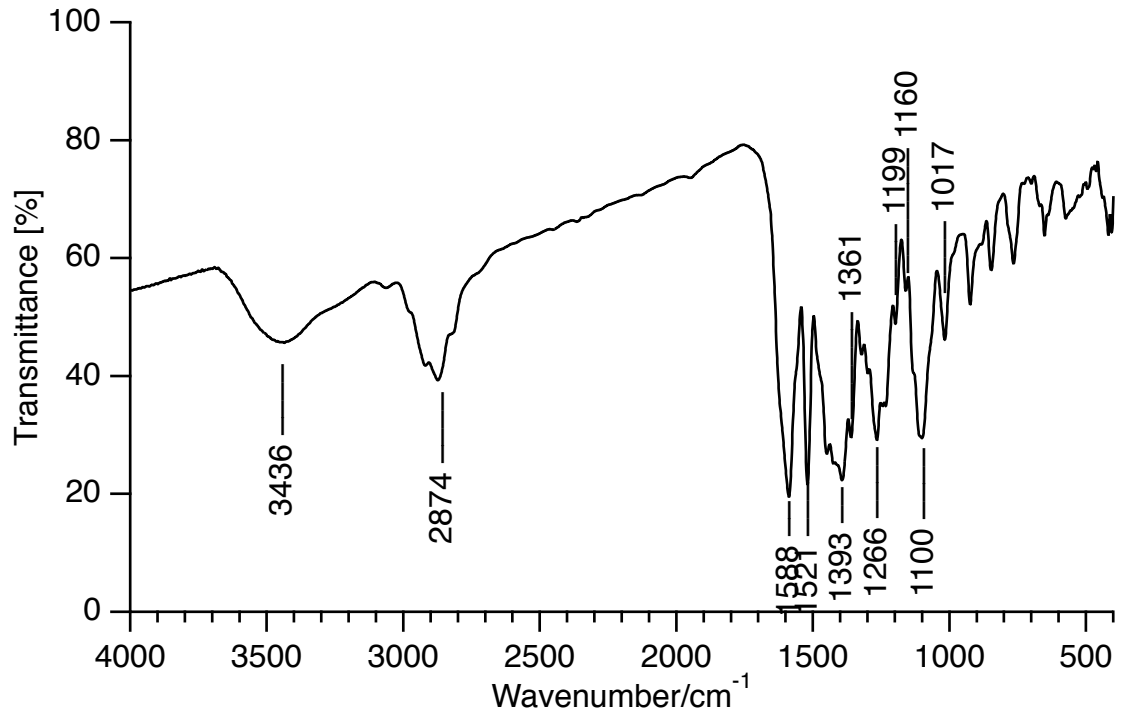

Figure S29. IR spectrum of [**1**$Zn_6(acac)_6$] (KBr).

A single crystal of **7** suitable for an X-ray diffraction analysis was obtained by the slow evaporation of a CH_2Cl_2/MeOH solution of **7**.

Crystal data for **7**: $C_{22}H_{20}N_2O_7$, *Fw* = 424.40, colorless plate, 0.50 × 0.08 × 0.06 mm^3, monoclinic, space group *P* $2_1/c$ (No. 14), *a* = 18.621(3) Å, *b* = 13.302(2) Å, *c* = 8.0510(140) Å, β = 91.298(8)°, *V* = 1993.7(6) Å^3, *Z* = 4, R_1 = 0.0836, wR_2 = 0.2333, GOF = 1.273.

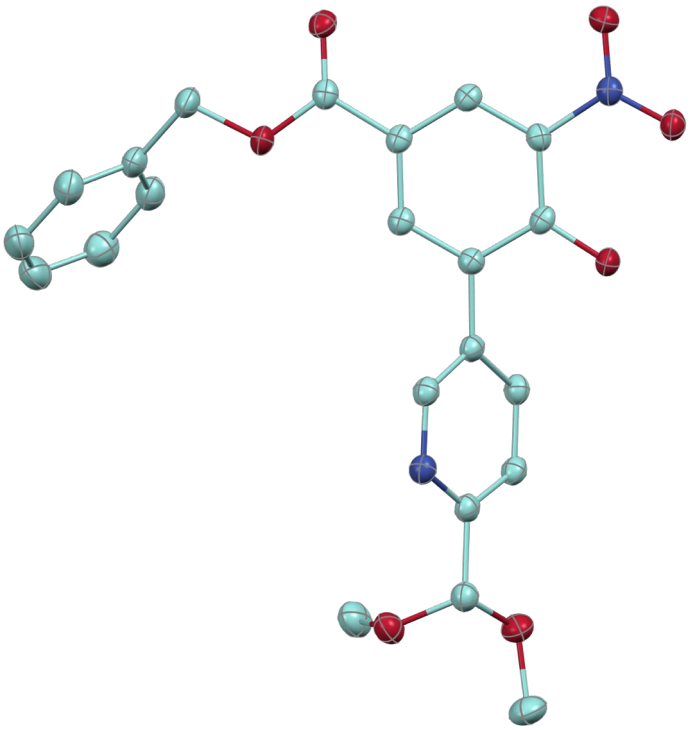

Figure S30. The molecular structure of **7** determined by X-ray diffraction analysis. An ellipsoidal model (50% probability). Hydrogen atoms were omitted for clarity. C, light green; N, blue; O, red.

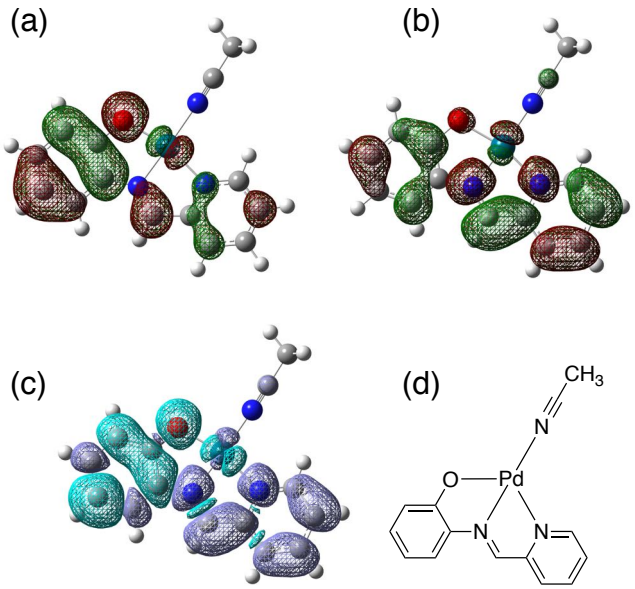

Figure S31. Molecular orbitals of $[Pd(pap)(CH_3CN)]^+$ obtained by DFT calculations. (a) HOMO. (b) LUMO. (c) The difference in electron density in HOMO→LUMO transition. (d) The structure of $[Pd(pap)(CH_3CN)]^+$. A TD-DFT calculation suggests that $[Pd(pap)(CH_3CN)]^+$ shows absorption at 581 nm with the oscillator strength f = 0.109 (HOMO→LUMO 97%).

Complexation of Pd-hexapap and pyridine derivatives

Scheme S10. Formation of [**1**Pd$_6$(tbp)$_6$](BF$_4$)$_6$ (tbp = 4-*tert*-butylpyridine)

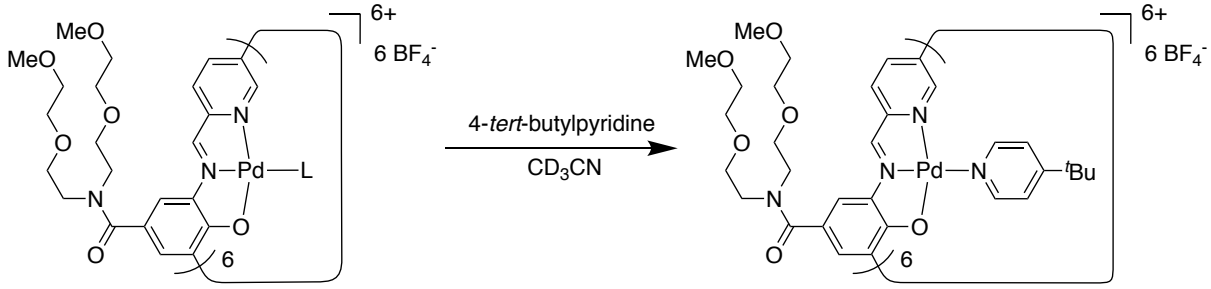

[**1**Pd$_6$L$_6$](BF$_4$)$_6$ [**1**Pd$_6$(tbp)$_6$](BF$_4$)$_6$

[**1**Pd$_6$](BF$_4$)$_6$·4MeCN·6H$_2$O·0.25Et$_2$O (6.19 mg, 1.51 μmol, 1.0 eq.) and 4-*tert*-butylpyridine (tbp) (1.25 mg, 9.24 μmol, 6.1 eq.) in a CD$_3$CN (500 μL) were mixed at room temperature. The complexation reaction was completed within 5 min and the formation of [**1**Pd$_6$(tbp)$_6$](BF$_4$)$_6$ was confirmed by ^{1}H NMR and ESI-MS measurements.

^{1}H NMR (600 MHz, CD$_3$CN): δ 8.55 (dd, *J* = 8.1, 1.2 Hz, 2H), 8.44 (d, *J* = 5.7 Hz, 4H), 8.33 (s, 2H), 8.30 (s, 2H), 8.29 (d, *J* = 1.7 Hz, 2H), 8.29 (s, 2H), 8.22 (dd, *J* = 8.4, 1.7 Hz, 2H), 8.17 (d, *J* = 1.2 Hz, 2H), 8.13 (dd, *J* = 7.8, 1.2 Hz, 2H), 8.13 (d, *J* = 6.9 Hz, 4H), 7.96 (d, *J* = 8.4 Hz, 2H), 7.95 (d, *J* = 7.8 Hz, 2H), 7.83 (d, *J* = 8.1 Hz, 2H), 7.77 (d, *J* = 1.6 Hz, 2H), 7.75 (d, *J* = 1.5 Hz, 2H), 7.69 (d, *J* = 1.2 Hz, 2H), 7.64 (d, *J* = 1.5 Hz, 2H), 7.60 (d, *J* = 5.7 Hz, 4H), 7.59 (d, *J* = 6.3 Hz, 4H), 7.57 (d, *J* = 1.6 Hz, 2H), 7.49 (d, *J* = 6.9 Hz, 4H), 7.48 (d, *J* = 6.3 Hz, 4H), 7.39 (d, *J* = 1.2 Hz, 2H), 7.28 (d, *J* = 1.2 Hz, 2H), 3.64–3.41 (96H), 3.28–3.21 (36H), 1.32 (s, 18H), 1.28 (s, 18H), 0.63 (s, 18H).

ESI-TOF MS *m*/*z* calcd for ([**1**Pd$_6$(tbp)$_6$]$^{6+}$): 684.04; found: 684.03.

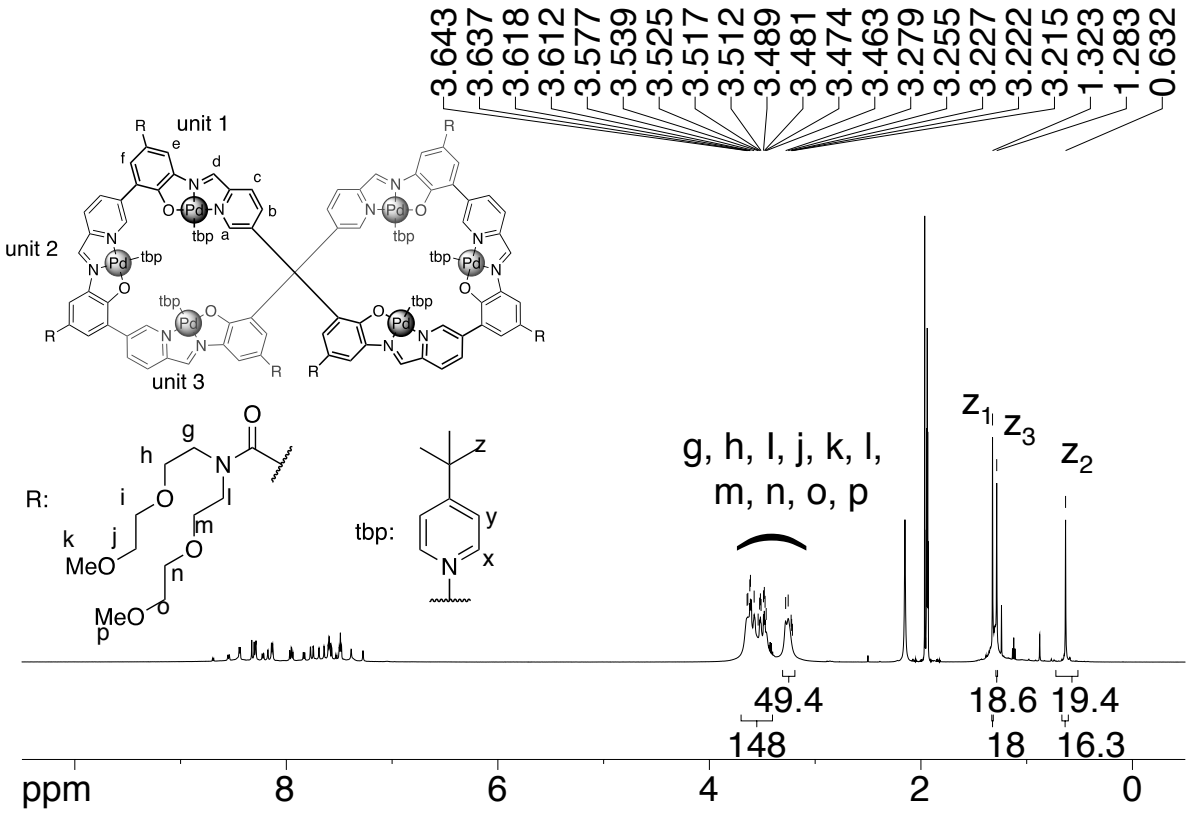

Figure S32. ^{1}H NMR spectrum of [**1**Pd$_6$(tbp)$_6$](BF$_4$)$_6$ (δ = –0.5 to 10.5 ppm) (600 MHz, CD$_3$CN).

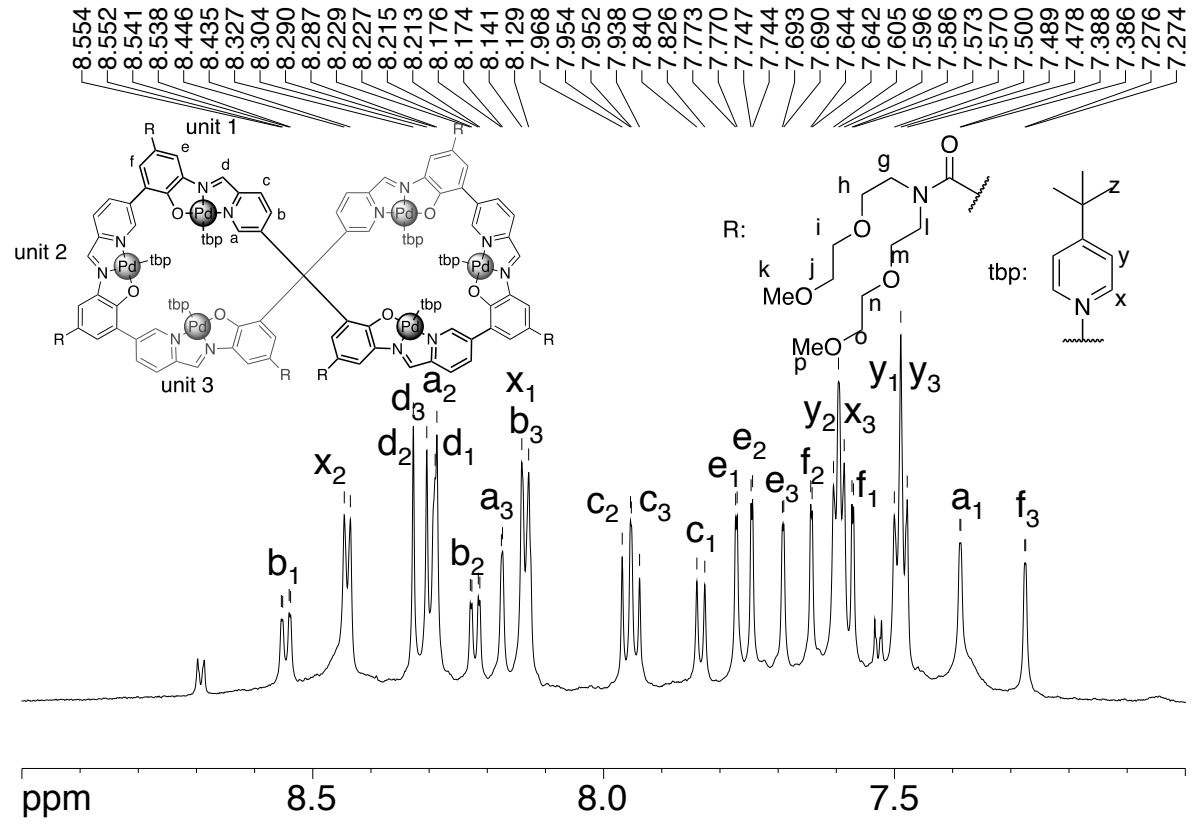

Figure S33. ^{1}H NMR spectrum of [**1**Pd$_6$(tbp)$_6$](BF$_4$)$_6$ (δ = 7.0 to 9.0ppm) (600 MHz, CD$_3$CN).

Table S1. Assignment of ^{1}H NMR signals and their chemical shifts (600 MHz, CD_3CN). δ_{CD3CN} [ppm]: A chemical shift of a proton signal of [**1**$Pd_6(NCCD_3)_6$]$(BF_4)_6$. δ_{tbp} [ppm]: A chemical shift of a proton signal of [**1**$Pd_6(tbp)_6$]$(BF_4)_6$. $\Delta\delta$ [ppm]: Difference in chemical shift between the two species (= $\delta_{tbp} - \delta_{CD3CN}$). The tables were shown in (a) an alphabetical order and (b) an ascending order ($\Delta\delta$), respectively.

(a) Alphabetical order

^{1}H	δ_{CD3CN} / ppm	δ_{tbp} / ppm	$\Delta\delta$ / ppm
a_1	8.51	7.39	-1.12
a_2	8.51	8.29	-0.22
a_3	8.51	8.18	-0.33
b_1	8.25	8.55	0.30
b_2	8.25	8.22	-0.03
b_3	8.25	8.14	-0.12
c_1	7.89	7.83	-0.06
c_2	7.89	7.96	0.07
c_3	7.89	7.95	0.06
d_1	8.20	8.29	0.09
d_2	8.20	8.33	0.13
d_3	8.20	8.30	0.10
e_1	7.74	7.77	0.03
e_2	7.74	7.75	0.00
e_3	7.74	7.69	-0.05
f_1	7.53	7.57	0.04
f_2	7.53	7.64	0.11
f_3	7.53	7.28	-0.26

(b) Ascending order

^1H	δ_{CD3CN} / ppm	δ_{tbp} / ppm	$\Delta\delta$ / ppm
a_1	8.51	7.39	-1.12
a_3	8.51	8.18	-0.33
f_3	7.53	7.28	-0.26
a_2	8.51	8.29	-0.22
b_3	8.25	8.14	-0.12
c_1	7.89	7.83	-0.06
e_3	7.74	7.69	-0.05
b_2	8.25	8.22	-0.03
e_2	7.74	7.75	0.00
e_1	7.74	7.77	0.03
f_1	7.53	7.57	0.04
c_3	7.89	7.95	0.06
c_2	7.89	7.96	0.07
d_1	8.20	8.29	0.09
d_3	8.20	8.30	0.10
f_2	7.53	7.64	0.11
d_2	8.20	8.33	0.13
b_1	8.25	8.55	0.30

Table S2. The chemical shifts of [**1**$Pd_6(tbp)_6$]$(BF_4)_6$ compared by each Pd(pap) unit (600 MHz, CD_3CN). δ_{tbp} [ppm]: A chemical shift of a proton signal of [**1**$Pd_6(tbp)_6$]$(BF_4)_6$. $R(\delta_{tbp})$ [ppm]: A difference between the maximum and minimum of chemical shifts of the three Pd(pap) units. $Q_{1/2}(\delta_{tbp})$ [ppm]: A median of chemical shifts of the three Pd(pap) units. The tables were shown in (a) an alphabetical order and (b) a descending order ($Q_{1/2}(\delta_{tbp}) - \delta_{tbp}$), respectively.

(a) Alphabetical order

^1H	$R(\delta_{tbp})$/ ppm	δ_{tbp} / ppm	($Q_{1/2}(\delta_{tbp})$-δ_{tbp})/ ppm
a_1	0.90	7.39	0.79
a_2		8.29	-0.11
a_3		8.18	0.00
b_1	0.41	8.55	-0.32
b_2		8.22	0.00
b_3		8.14	0.09
c_1	0.13	7.83	0.11
c_2		7.96	-0.02
c_3		7.95	0.00
d_1	0.04	8.29	0.02
d_2		8.33	-0.02
d_3		8.30	0.00
e_1	0.08	7.77	-0.03
e_2		7.75	0.00
e_3		7.69	0.05
f_1	0.37	7.57	0.00
f_2		7.64	-0.07
f_3		7.28	0.30

(b) Descending order

^1H	δ_{tbp} / ppm	$(Q_{1/2}(\delta_{tbp})-\delta_{tbp})$/ ppm
a_1	7.39	0.79
f_3	7.28	0.30
c_1	7.83	0.11
b_3	8.14	0.09
e_3	7.69	0.05
d_1	8.29	0.02
a_3	8.18	0.00
b_2	8.22	0.00
c_3	7.95	0.00
d_3	8.30	0.00
e_2	7.75	0.00
f_1	7.57	0.00
c_2	7.96	-0.02
d_2	8.33	-0.02
e_1	7.77	-0.03
f_2	7.64	-0.07
a_2	8.29	-0.11
b_1	8.55	-0.32

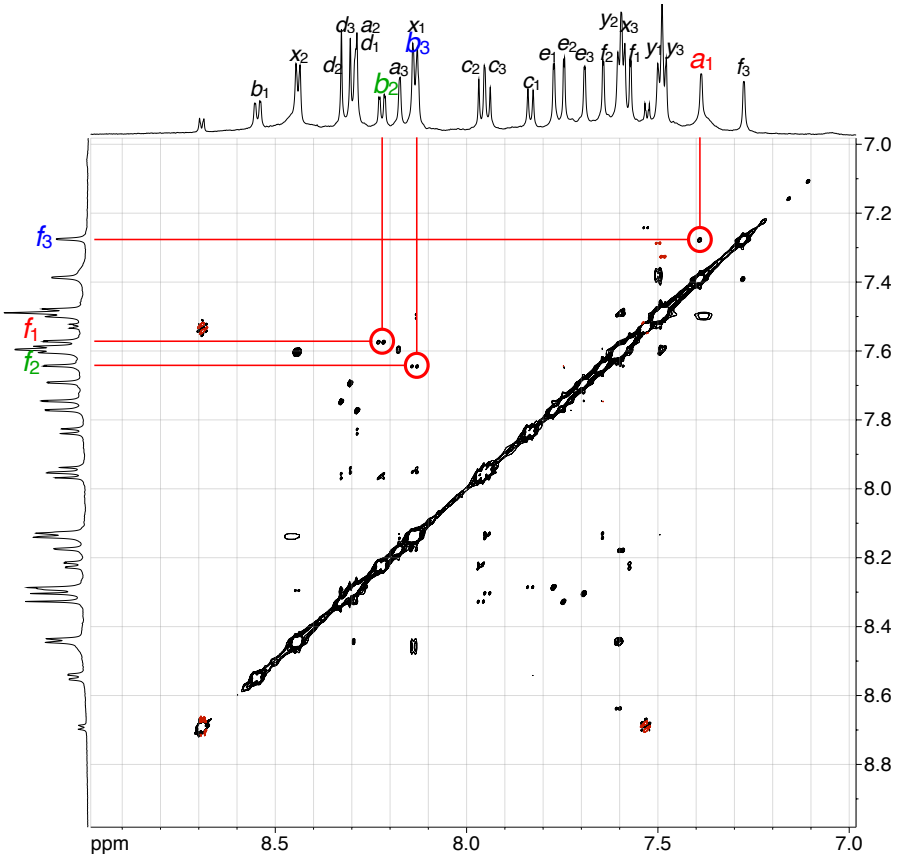

Figure S34. ^{1}H–^{1}H NOESY spectrum of [**1**Pd$_6$(tbp)$_6$](BF$_4$)$_6$ (600 MHz, CD$_3$CN, 298 K).

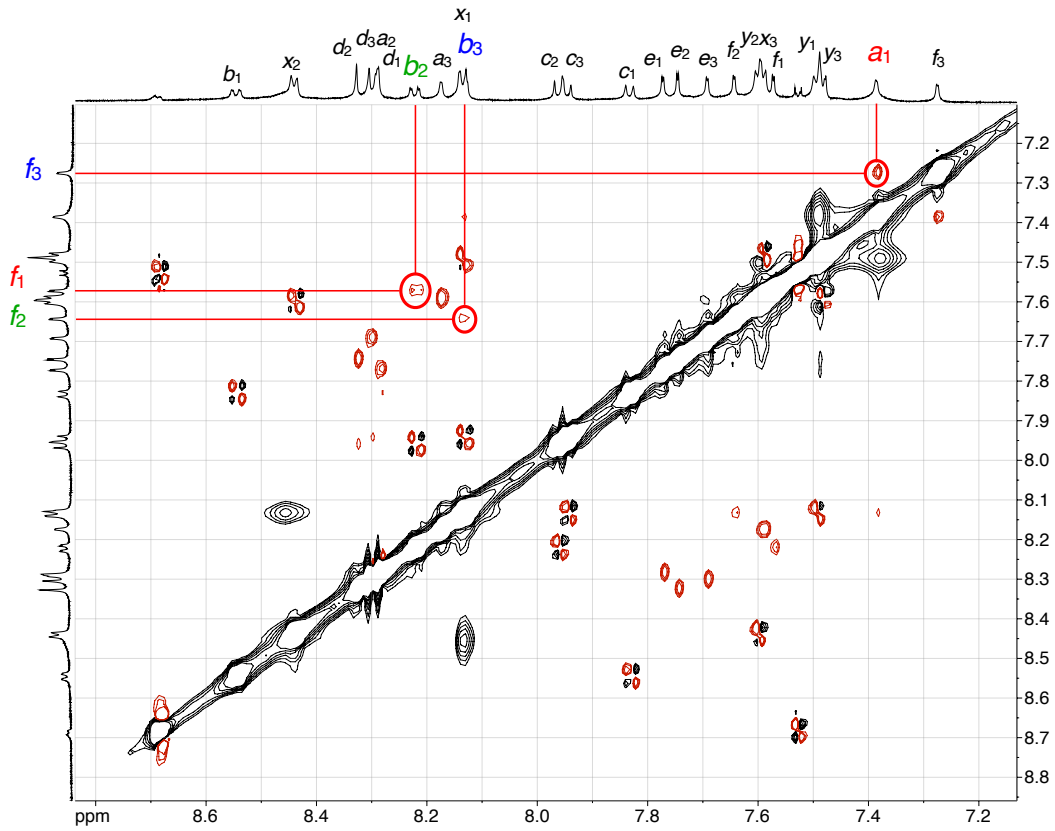

Figure S35. ^{1}H–^{1}H ROESY spectrum of [**1**Pd$_6$(tbp)$_6$](BF$_4$)$_6$ (600 MHz, CD$_3$CN, 298 K).

MM calculation of [1´Pd$_6$(tbp)$_6$]$^{6+}$

The conformational search of [**1**´Pd$_6$(tbp)$_6$]$^{6+}$ was performed as follows. A C_6-symmetric planar conformation of [**1**´Pd$_6$(tbp)$_6$]$^{6+}$ was used as an initial structure for the MM calculation. Each atom of the first initial structure was moved in such a way as to add a normal random number (average: 0 Å, standard deviation: 0.2 Å) to the atom's Cartesian coordinate (x,y,z). The normal random number was generated by Box–Muller's method[S11]. The generated disarranged structure was put into MM calculation to obtain the first energy-minimized structure. During this first optimization, two provisional hydrogen atoms were put on the axial positions of each [Pd(pap)(tbp)]$^+$ unit to make an octahedral hexacoordinate center so as to fix the coordination geometry of the [Pd(pap)(tbp)]$^+$ part into square-planar. The UFF force field was used, and the electronic charge was not applied in this calculation. Then, the second initial structure of [**1**´Pd$_6$(tbp)$_6$]$^{6+}$ was generated from the first optimized structure by eliminating the provisional hydrogens, and was optimized by MM calculation to obtain the second energy-minimized structure. The total net charge was set to 6+, which was assigned by QEq method during the second calculation.

The final optimized structure was obtained as the most stable structure from the 10,000 calculations as described above (4,576 entries were converged among the 10,000 trials). The calculated structure of [**1**´Pd$_6$(tbp)$_6$]$^{6+}$ has an approximate C_2-symmetric twisted framework that is consistent with NOESY and ROESY experiments.

(a)

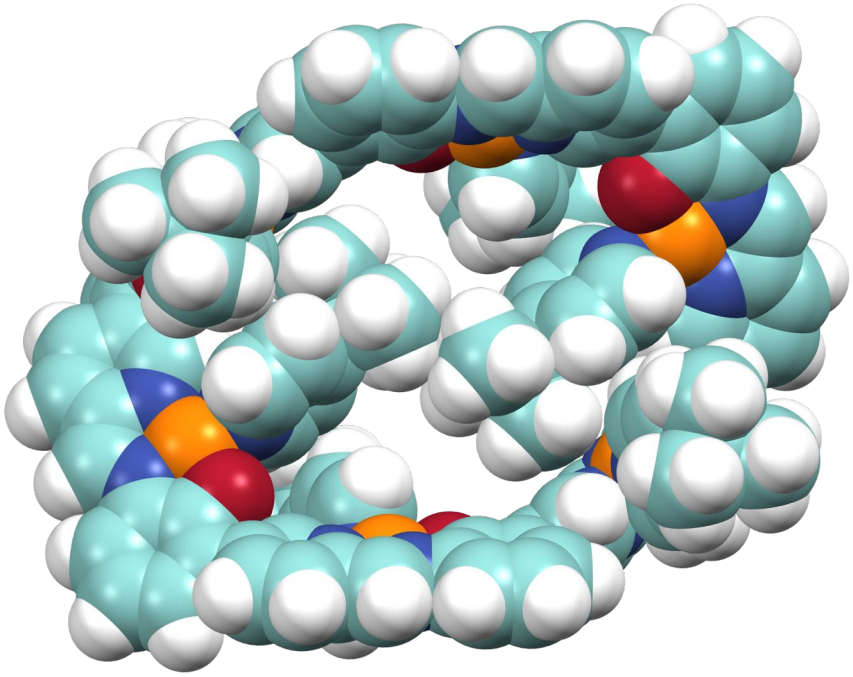

(b)

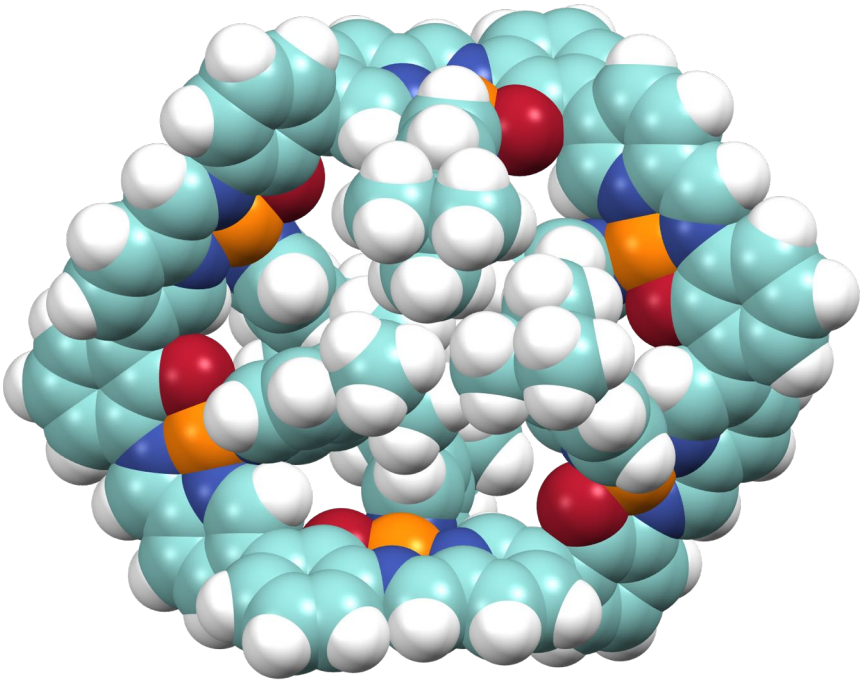

Figure S36. Comparison of the energy-minimized structures of [**1**´$Pd_6(tbp)_6$]$^{6+}$ obtained by molecular mechanics calculations (H_6**1**´: R = H in the structure of H_6**1**). A space filling model. C, light green; N, blue; O, red; H, white; Pd, orange. (a) C_2-symmetric conformation. (b) C_i-symmetric conformation. The C_2-symmetric structure (a) is more stable by 38 kJ/mol than the C_i-symmetric structure (b).

Evaluation of the calculated structure of [1′Pd$_6$(tbp)$_6$]$^{6+}$ using NOESY

To evaluate the calculated structure of [**1**′Pd$_6$(tbp)$_6$]$^{6+}$ with the NOESY experiment of [**1**Pd$_6$(tbp)$_6$]$^{6+}$, the distances d between the proton pairs (f_1, b_2), (f_2, b_3), and (f_3, a_1) in the calculated structure and the ones estimated from the NOE strengths were compared.

The distances d estimated from the NOE strengths were calculated using the expression (1) between I (intensity of NOE between two protons) and d (distance between the corresponding protons).[S12]

$$I = \frac{A}{d^6} \quad \text{—(1)}$$

The proportionality constant A was determined from the NOE intensities of intraunit proton pairs ((c,d) and (d,e)) and the distances between the corresponding protons in the calculated structure (Table S3). The calculated structure takes an approximate C_2-symmetry but the corresponding diagonal units are not exactly identical. Thus, the averaged values shown in the equation (2) was used as the distance d.

$$Average = \left(\frac{1}{n} \sum_{i=1}^{n} d_i^{-6} \right)^{-\frac{1}{6}} \quad \text{—(2)}$$

Then, the distances between the interunit proton pairs were estimated using thus obtained A and the observed NOE intensities. As shown in Table S3, the distances estimated from NOE matched well with those of the MM-calculated structure.

Table S3. Comparison of the distances between protons of the MM-calculated structure of [**1**′Pd$_6$(tbp)$_6$]$^{6+}$ and those estimated from the NOESY measurement of [**1**Pd$_6$(tbp)$_6$]$^{6+}$

			d [Å] (MM)			*I* [a.u.] (NOESY)			*A* (Proportionality constant)	averaged *A* (arithmetical mean)
			1–3	1′–3′	Average	top left	bottom right	arithmetical mean		
Intraunit	Unit 1	c–d	2.669	2.672	2.671	2.14E+06	1.77E+06	1.96E+06	7.094E+08	**7.739E+08**
		d–e	2.393	2.399	2.396	4.14E+06	4.18E+06	4.16E+06	7.874E+08	
	Unit 2	c–d	2.686	2.693	2.689	2.10E+06	2.03E+06	2.07E+06	7.813E+08	
		d–e	2.405	2.400	2.402	3.82E+06	4.10E+06	3.96E+06	7.611E+08	
	Unit 3	c–d	2.671	2.665	2.668	2.27E+06	2.13E+06	2.20E+06	7.941E+08	
		d–e	2.388	2.384	2.386	4.23E+06	4.56E+06	4.40E+06	8.103E+08	
									d [Å] (NOE)	
Interunit	Unit 1–2 (*f*–*b*)		2.591	2.636	**2.613**	2.59E+06	2.70E+06	2.65E+06	**2.577**	
	Unit 2–3 (*f*–*b*)		2.599	2.543	**2.570**	2.46E+06	2.54E+06	2.50E+06	**2.601**	
	Unit 3–1 (*f*–*a*)		2.549	2.537	**2.543**	2.57E+06	2.44E+06	2.51E+06	**2.600**	

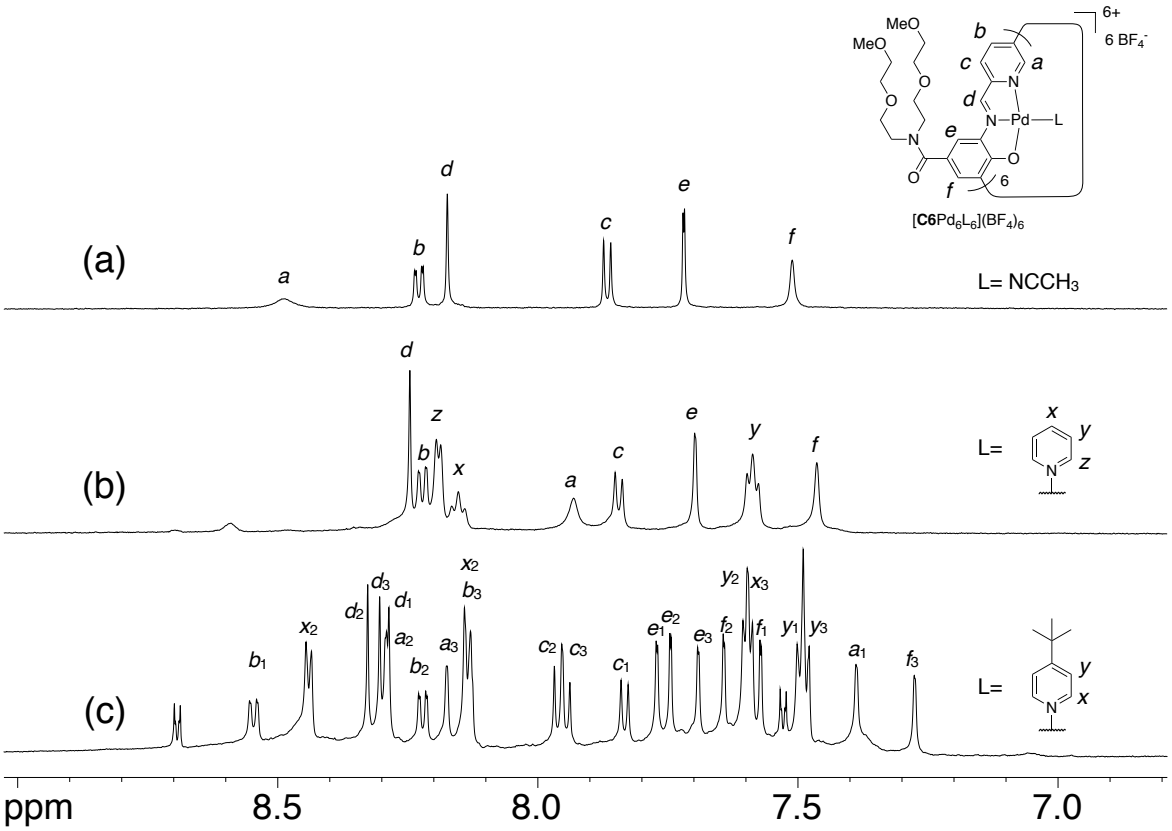

Figure S37. Comparison of ^{1}H NMR spectra [**1**Pd$_6$L$_6$](BF$_4$)$_6$ with pyridine derivatives (600 MHz, CD$_3$CN, 298 K). (a) [**1**Pd$_6$(CD$_3$CN)$_6$](BF$_4$)$_6$. (b) [**1**Pd$_6$(py)$_6$](BF$_4$)$_6$. (c) [**1**Pd$_6$(tbp)$_6$](BF$_4$)$_6$.

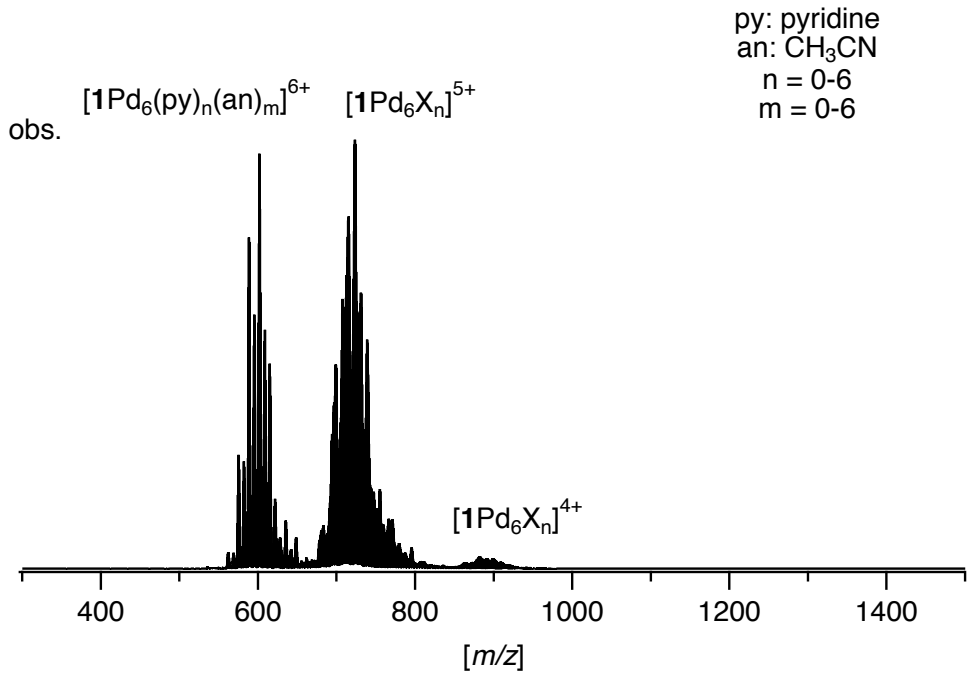

Figure S38. ESI-TOF mass spectrum of [**1**Pd$_6$(py)$_6$](BF$_4$)$_6$. (*m*/*z* = 300–1500) (CH$_3$CN, positive).

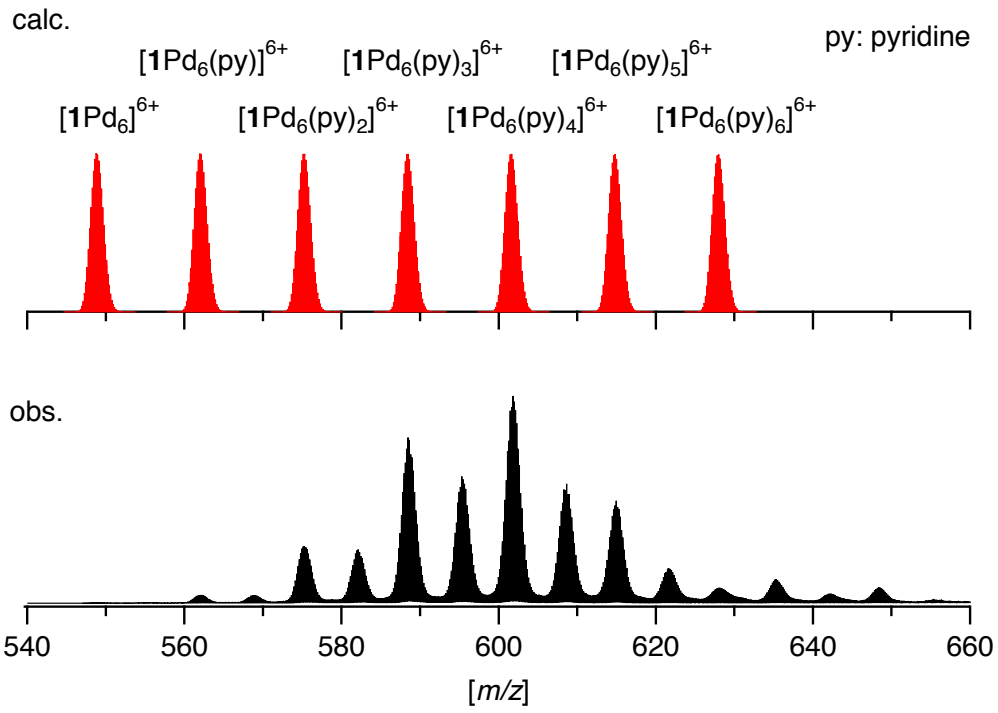

Figure S39. ESI-TOF mass spectrum of $[\mathbf{1}Pd_6(py)_6](BF_4)_6$. ($m/z$ = 540–660) (CH_3CN, positive).

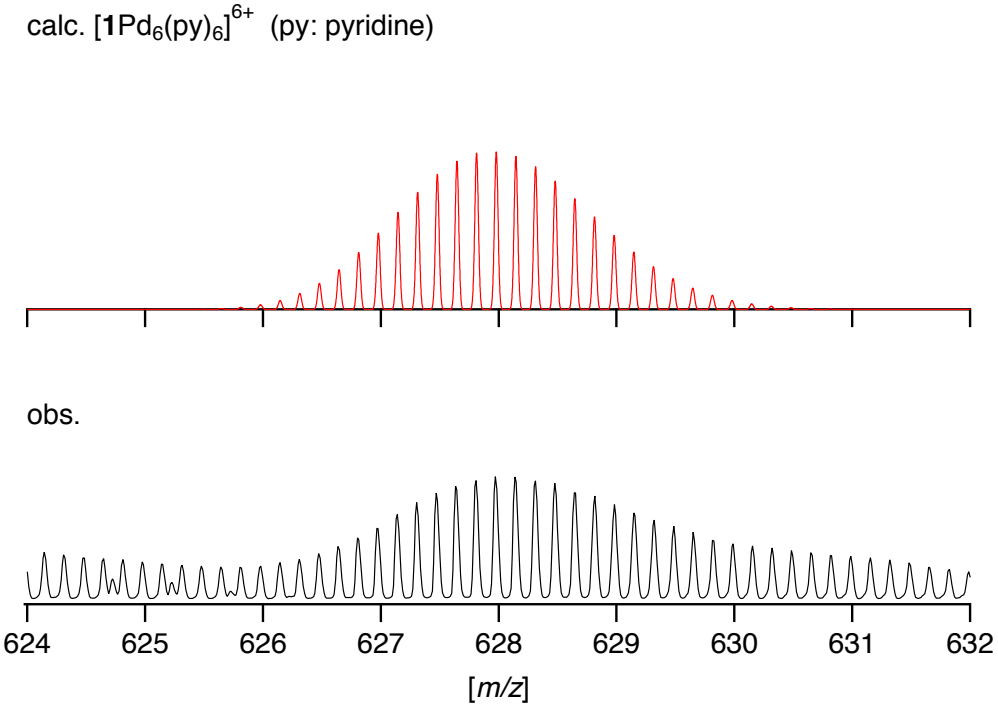

Figure S40. ESI-TOF mass spectrum of $[\mathbf{1}Pd_6(py)_6](BF_4)_6$. ($m/z$ = 624–632) (CH_3CN, positive).

Table S4. The chemical shifts of [**1**$Pd_6(py)_6$]$(BF_4)_6$ compared to those of [**1**$Pd_6(tbp)_6$]$(BF_4)_6$(600 MHz, CD_3CN). δ_{py} [ppm]: A chemical shift of a proton signal of [**1**$Pd_6(py)_6$]$(BF_4)_6$. δ_{tbp} [ppm]: A chemical shift of a proton signal of [**1**$Pd_6(tbp)_6$]$(BF_4)_6$. *Ave*(δ_{tbp}) [ppm]: An average of chemical shifts of the three Pd(pap) units of [**1**$Pd_6(tbp)_6$]$(BF_4)_6$.

^1H	δ_{py} / ppm	δ_{tbp} / ppm	*Ave*(δ_{tbp}) / ppm
a_1	7.93	7.39	7.95
a_2		8.29	
a_3		8.18	
b_1	8.22	8.55	8.30
b_2		8.22	
b_3		8.14	
c_1	7.85	7.83	7.91
c_2		7.96	
c_3		7.95	
d_1	8.25	8.29	8.31
d_2		8.33	
d_3		8.30	
e_1	7.70	7.77	7.74
e_2		7.75	
e_3		7.69	
f_1	7.46	7.57	7.50
f_2		7.64	
f_3		7.28	

The chemical shift value of each ^1H NMR signal of [**1**$Pd_6(py)_6$]$(BF_4)_6$ was similar to the averaged values of the three corresponding protons of [**1**$Pd_6(tbp)_6$]$(BF_4)_6$, thus it is probable that [**1**$Pd_6(py)_6$]$(BF_4)_6$ has a C_2-symmetric scaffold as [**1**$Pd_6(tbp)_6$]$(BF_4)_6$.

Interaction of Δ-TRISPHAT anion with [1Pd$_6$(tbp)$_6$]$^{6+}$

[**1**Pd$_6$](BF$_4$)$_6$·4MeCN·6H$_2$O·0.25Et$_2$O (6.05 mg, 1.47 μmol, 1.0 eq.) and 4-*tert*-butylpyridine (1.5 μL, 10.2 μmol, 6.9 eq.) in a CD$_3$CN (100 μL) was mixed with Δ-TRISPHAT tetrabutylammonium salt (1.5 μmol, 1.0 eq.) in CD$_3$CN (100 μL), followed by the addition of CD$_3$CN (300 μL). The sample was analyzed by ^{1}H NMR, UV-vis absorption, and circular dichroism measurements.

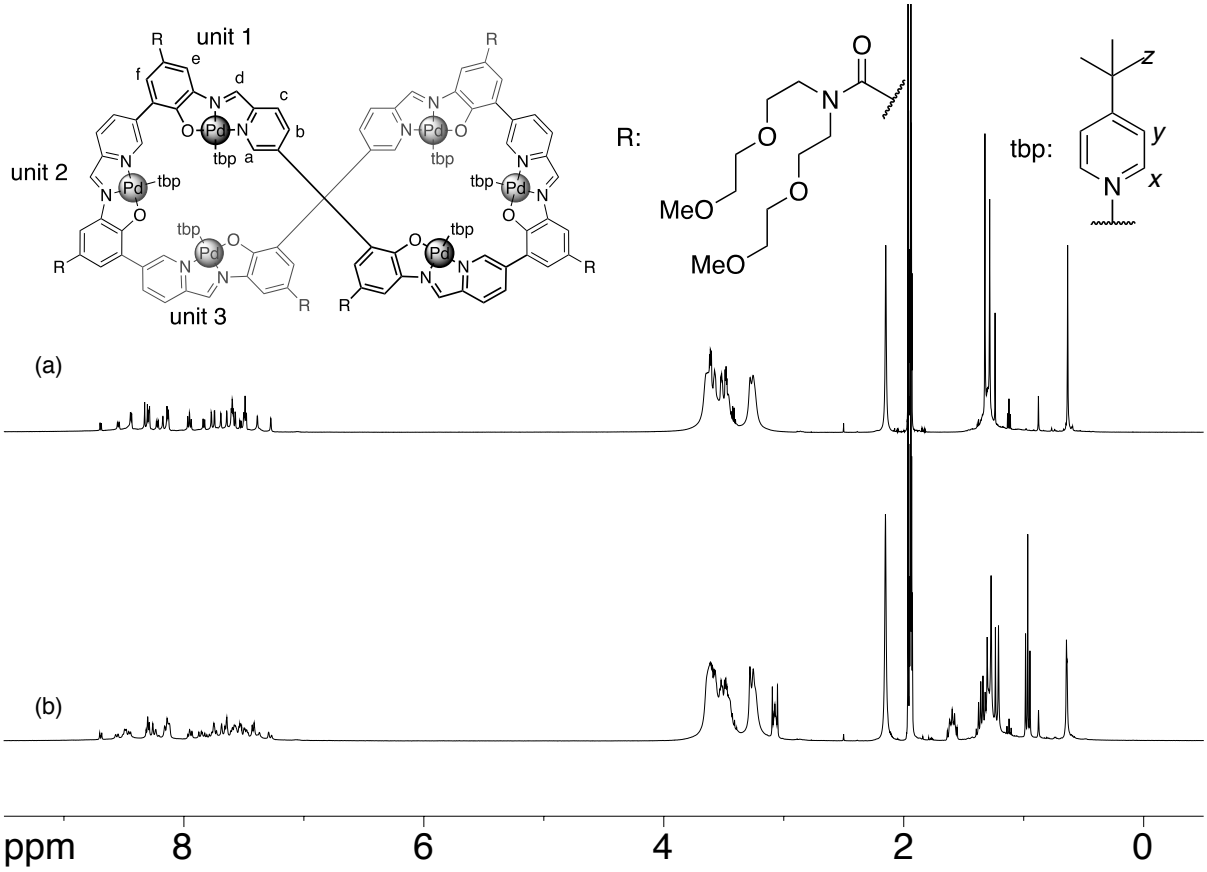

Figure S41. Interaction of Δ-TRISPHAT anion with [**1**Pd$_6$(tbp)$_6$]$^{6+}$ (–0.5 to 9.5 ppm) (^{1}H NMR, 400 MHz, CD$_3$CN). (a) [**1**Pd$_6$(tbp)$_6$](BF$_4$)$_6$. (b) [**1**Pd$_6$(tbp)$_6$](BF$_4$)$_6$ + (*n*-Bu$_4$N)(Δ-TRISPHAT) (1.0 eq).

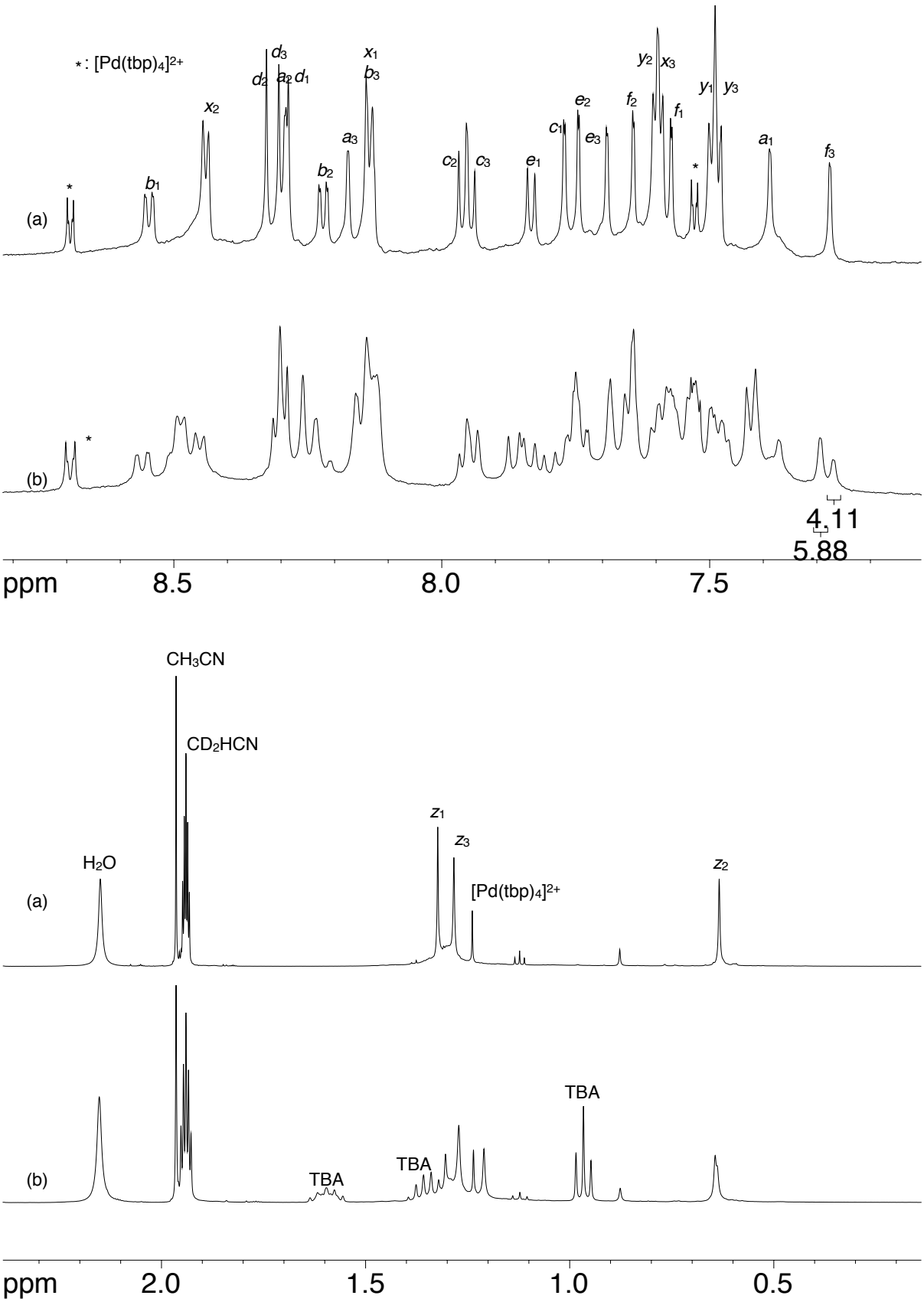

Figure S42. Interaction of Δ-TRISPHAT anion with $[\mathbf{1}Pd_6(tbp)_6]^{6+}$ (7.1 to 8.8 ppm, 0.2 to 2.3 ppm) (^{1}H NMR, 400 MHz, CD_3CN). (a) $[\mathbf{1}Pd_6(tbp)_6](BF_4)_6$. (b) $[\mathbf{1}Pd_6(tbp)_6](BF_4)_6$ + (*n*-Bu_4N)(Δ-TRISPHAT) (1.0 eq) (TBA: tetrabutylammonium).

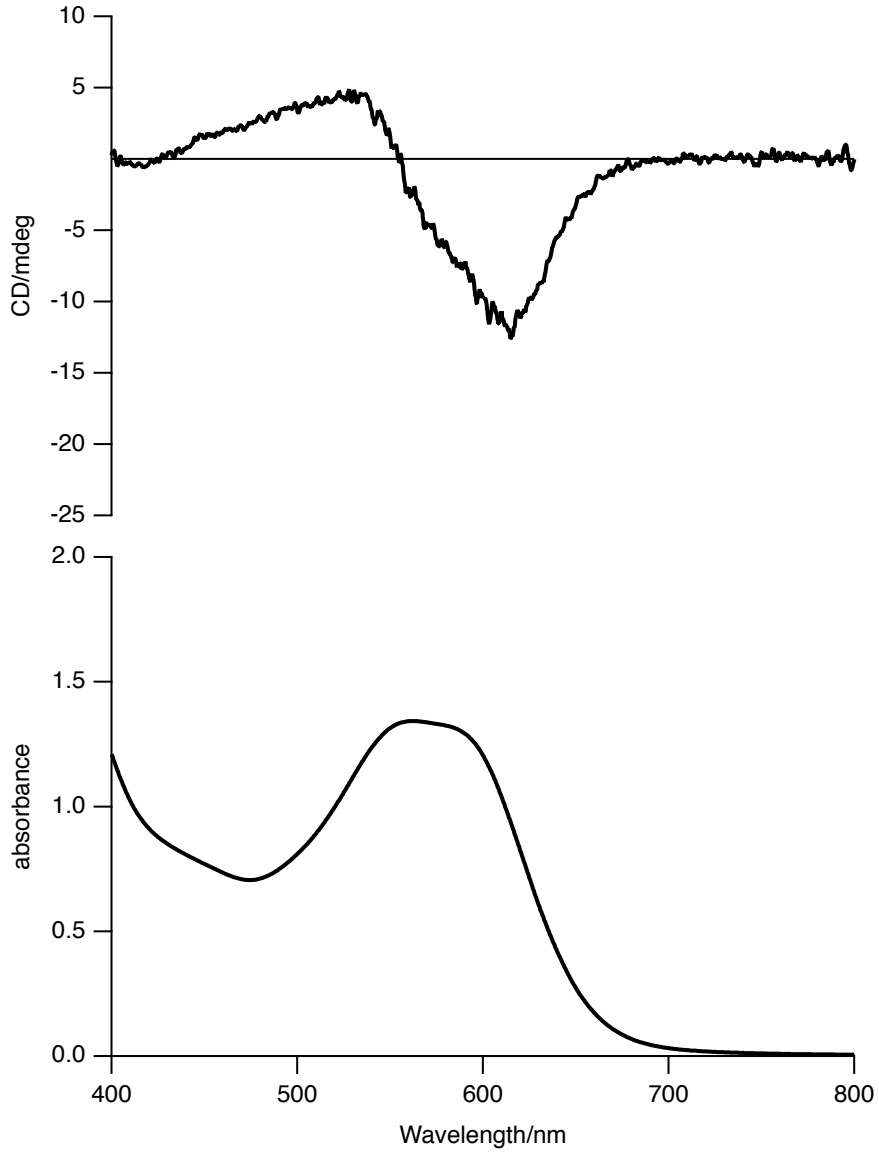

Figure S43. Circular dichroism (top) and UV/vis absorption (bottom) spectra of a 1:1 mixture of [**1**$Pd_6(tbp)_6$]$(BF_4)_6$ and (*n*-Bu_4N)(Δ-TRISPHAT) (CH_3CN, 29 μM, 298 K, *l* = 1 cm).

References for the Supplementary Information

1. G. R. Fulmer, A. J. M. Miller, N. H. Sherden, H. E. Gottlieb, A. Nudelman, B. M. Stoltz, J. E. Bercaw and K. I. Goldberg, *Organometallics*, 2010, **29**, 2176–2179.
2. G. M. Sheldrick, *Acta Cryst.*, 2008, **A64**, 112–122.
3. G. M. Sheldrick, *Acta Cryst.*, 2015, **C71**, 3–8.
4. (a) K. Wakita, *Yadokari-XG, Software for Crystal Structure Analyses*, (2001); (b) C. Kabuto, S. Akine, T. Nemoto and E. Kwon, *J. Cryst. Soc. Jpn.*, 2009, **51**, 218–224.
5. M. J. Frisch, G. W. Trucks, H. B. Schlegel, G. E. Scuseria, M. A. Robb, J. R. Cheeseman, G. Scalmani, V. Barone, G. A. Petersson, H. Nakatsuji, X. Li, M. Caricato, A. V. Marenich, J. Bloino, B. G. Janesko, R. Gomperts, B. Mennucci, H. P. Hratchian, J. V. Ortiz, A. F. Izmaylov, J. L. Sonnenberg, D. Williams-Young, F. Ding, F. Lipparini, F. Egidi, J. Goings, B. Peng, A. Petrone, T. Henderson, D. Ranasinghe, V. G. Zakrzewski, J. Gao, N. Rega, G. Zheng, W. Liang, M. Hada, M. Ehara, K. Toyota, R. Fukuda, J. Hasegawa, M. Ishida, T. Nakajima, Y. Honda, O. Kitao, H. Nakai, T. Vreven, K. Throssell, J. A. Montgomery, Jr., J. E. Peralta, F. Ogliaro, M. J. Bearpark, J. J. Heyd, E. N. Brothers, K. N. Kudin, V. N. Staroverov, T. A. Keith, R. Kobayashi, J. Normand, K. Raghavachari, A. P. Rendell, J. C. Burant, S. S. Iyengar, J. Tomasi, M. Cossi, J. M. Millam, M. Klene, C. Adamo, R. Cammi, J. W. Ochterski, R. L. Martin, K. Morokuma, O. Farkas, J. B. Foresman and D. J. Fox, *Gaussian 16*, Revision A.03, Gaussian, Inc., Wallingford CT, 2016.
6. A. K. Rappé, C. J. Casewit, K. S. Colwell, W. A. G. III and W. M. Skiff, *J. Am. Chem. Soc.*, 1992, **114**, 10024–10035.
7. A. K. Rappe and W. A. Goddard III, *J. Phys. Chem.* 1991, **95**, 3358–3363.
8. G. W. K. Cavill, *J. Chem. Soc. Ind. London* 1945, **64**, 212−215.
9. A. Ojida, T. Sakamoto, M. Inoue, S. Fujishima, G. Lippens and I. Hamachi, *J. Am. Chem. Soc.*, 2009, **131**, 6543–6548.
10. C. Selve, J-C. Ravey, M-J. Stebe, C. El Moudjahid, E. M. Moumni and J-J. Delpuech, *Tetrahedron*, 1991, **47**, 411–428.
11. G. E. P. Box and M. E. Muller, *Ann. Math. Statist.*, 1958, **29**, 610–611.
12. T. D. W. Claridge, *High-Resolution NMR Techniques in Organic Chemistry*, Elsevier, Oxford, 1999.